

U.S. DEPARTMENT OF THE INTERIOR  
U.S. GEOLOGICAL SURVEY

**Seismic velocities and geologic logs from boreholes  
at three downhole arrays in San Francisco, California**

by

James F. Gibbs, Thomas E. Fumal, Roger D. Borchardt,  
Richard E. Warrick, Hsi-Ping Liu and Robert E. Westerlund <sup>1</sup>

**Open-File Report OF 94 - 706**

This report is preliminary and has not been reviewed for conformity with U.S. Geological Survey editorial standards or with the North American Stratigraphic Code. Any use of trade, product, or firm names is for descriptive purposes only and does not imply endorsement by the U.S. Government.

---

<sup>1</sup> U.S. Geological Survey, MS 977, Menlo Park, CA 94025

## TABLE OF CONTENTS

	Page
Introduction . . . . .	1
Field Techniques . . . . .	4
Drilling and Sampling Procedures . . . . .	4
Geologic Logs . . . . .	4
Travel-time Measurement Procedures . . . . .	5
Velocity Determinations . . . . .	6
Results . . . . .	8
Lithologic Logs . . . . .	8
S-wave Velocities . . . . .	9
P-wave Velocities . . . . .	9
Acknowledgments . . . . .	12
References . . . . .	13
Appendices--Detailed Results:	
Explanation of Geologic Logs . . . . .	14
Bessie Charmichael School . . . . .	15
S-Wave Table A1a . . . . .	22
P-Wave Table A1b . . . . .	23
Embarcadero Plaza . . . . .	24
S-Wave Table B1a . . . . .	31
P-Wave Table B1b . . . . .	32
Levi Plaza . . . . .	33
S-Wave Table C1a . . . . .	39
P-Wave Table C1b . . . . .	40

Seismic velocities and geologic logs from boreholes  
at three downhole arrays in San Francisco, California

by

James F. Gibbs, Thomas E. Fumal, Roger D. Borcherdt,  
Richard E. Warrick, Hsi-Ping Liu and Robert E. Westerlund

INTRODUCTION

The Loma Prieta earthquake of October 17, 1989 (1704 PST), has reinforced observations made by Wood et al., (1908) after the 1906 San Francisco earthquake, that poor ground conditions (soft soil) increase the likelihood of shaking damage to structures. Since 1908 many studies (e.g. Borcherdt, 1970, Borcherdt and Gibbs, 1976, Borcherdt and Glassmoyer, 1992) have shown that soft soils amplify seismic waves at frequencies that can be damaging to structures.

Damage in the City of San Francisco from the Loma Prieta earthquake was concentrated in the Marina District, the Embarcadero and the China Basin areas. Each of these areas, to some degree, are underlain by soft soil deposits. These concentrations of damage raise important questions regarding the amplification effects of such deposits at damaging levels of motion. Unfortunately, no strong-motion recordings were obtained in these areas during the Loma Prieta earthquake and only a limited number ( $< 10$ ) have been obtained on other soft soil sites in the United States. Consequently, important questions exist regarding the response of such deposits during damaging earthquakes, especially questions regarding the nonlinear soil response. Towards developing a data set to address these important questions, borehole strong-motion arrays have been installed at three locations. These arrays consist of groups of wide-dynamic-range pore-pressure transducers and three-component accelerometers, the outputs of which are recorded digitally. The arrays are designed to provide an integrated set of data on ground shaking, liquefaction-induced ground failure, and structural response. This report describes the detailed geologic, seismic, and material-property determinations derived at each of these sites. Locations of the sites are shown in Figure 1.



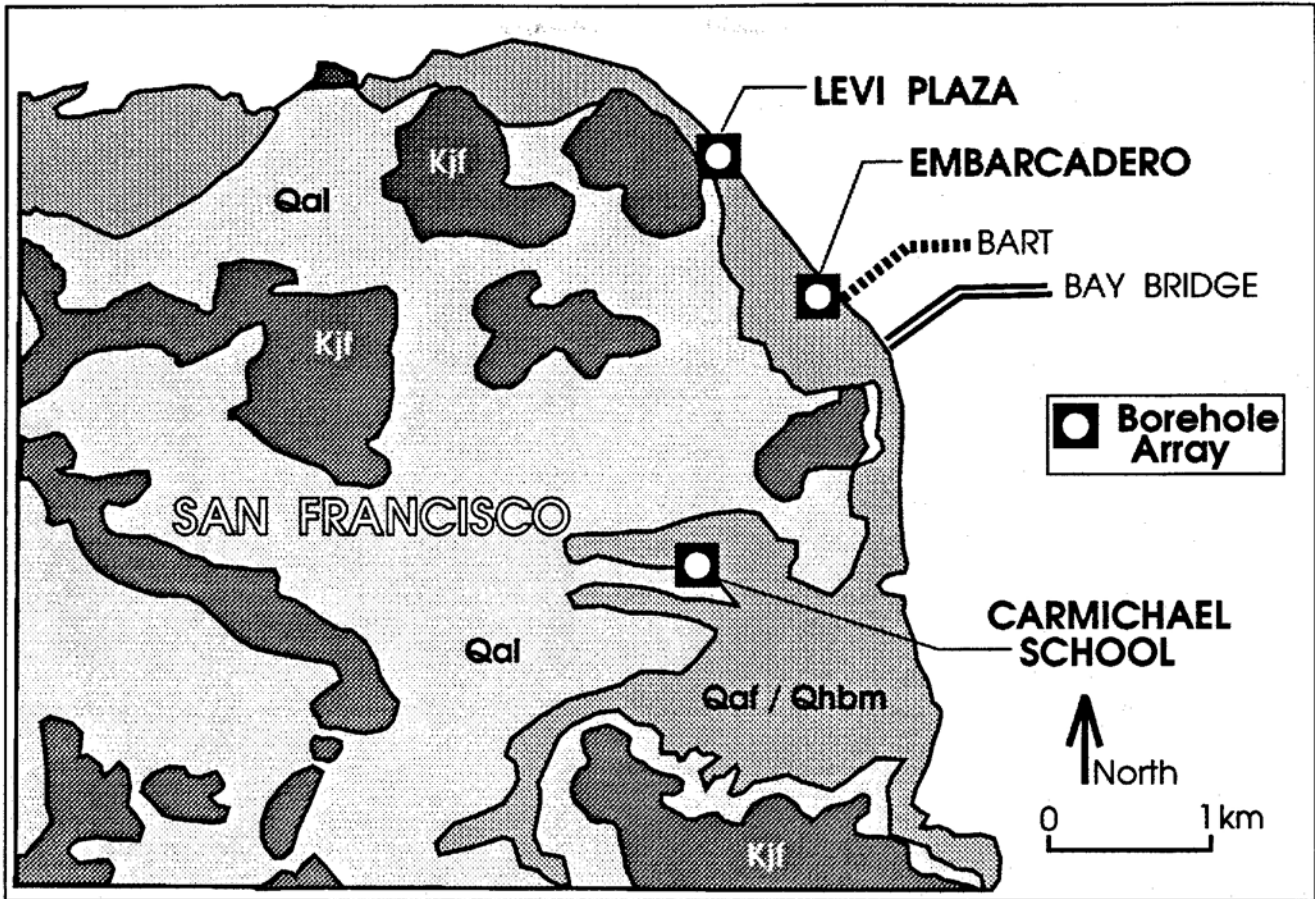


Figure 1b. Location map for borehole strong-motion arrays in San Francisco shown in relation to the distribution of geologic deposits. Explanation of the simplified geology shown by the stippling: Qaf (artificial fill), Qal (alluvium), Qhbm (Holocene Bay Mud), and Kjf (Franciscan Formation).

## FIELD TECHNIQUES

### Drilling and Sampling Procedures

At each site a pilot hole approximately 5 inches in diameter was drilled using rotary wash drilling with bentonite mud. Because of increased costs, core samples were not taken at these sites.

After completion of the pilot holes, the holes were reamed to 8 inches and were cased with 4-inch-inside-diameter, class-200, polyvinyl-chloride pipe, capped at the bottom.

The annular space around the casing was tremie grouted by pumping a water-cement-bentonite mixture through a 1-inch steel pipe lowered next to the casing. This provides good coupling between the casing and the wall of the borehole, and provides a sanitary seal preventing contamination of ground water. Grouting was done in stages of about 50-60 meters to prevent collapse of the casing. At this point, the boreholes are ready for installation of wide-dynamic-range accelerometers (at four depths, including one at the surface) and pore-pressure transducers (at two depths) at each location (Borcherdt et al., 1994).

### Geologic Logs

Geologic logs are based on descriptions of drill cuttings, reaction of the drill rig, and inspection of nearby outcrops. Drill cuttings are described using the field techniques of the Soil Conservation Service (1951). Descriptions include sediment texture, color, and the amount and size of coarse fragments. Texture refers to the relative proportions of clay, silt, and sand particles less than 2 millimeters in diameter. This is determined visually and by feel without using laboratory tests by the on-site geologist. As such, this system is easier to use in the field than other classification systems. The dominant color of the sediment and prominent mottles are determined from the Munsell soil color charts.

Most information needed for describing relatively well-sorted soils and such properties of rock as lithology, color, and hardness are readily obtained from cuttings. Inspection of nearby outcrops is necessary for determining the nature of poorly-sorted materials and fracture spacing. Reaction of the drill rig is useful in determining approximate sediment texture and in determining degree of fracturing because the rate of penetration in rock is highest for very closely fractured and crushed materials and drilling roughness generally

is at a maximum in closely to moderately fractured rock. In-situ consistency of soil is determined largely from standard penetration measurements and rate of drill penetration.

### Travel-time Measurement Procedures

Shear waves\* were generated at the ground surface by an air-powered horizontal hammer (Liu, et al., 1988) striking anvils attached to the ends of a 2.3-meter-long aluminum channel. The hammer can be driven in opposite horizontal directions to generate positive and negative shear pulses. A piezo-electric sensor attached to the shear source triggers the recorder for zero time. The source is offset from the borehole to prevent the direct arrival from traveling down the grout next to the casing. Offset distance is 2 to 5 meters depending on the depth of the borehole. Shallow holes (30 meters or less) are generally offset 2 meters, while boreholes deeper than approximately 100 meters are offset 3 to 5 meters. Travel-times are corrected (for slant offset) to vertical by the cosine of the angle of ray incidence. That is

$$t_c = t_m \cos(\alpha)$$

where:  $t_c$  = corrected travel-time,  $t_m$  = measured travel-time, and  $\alpha$  is the angle of incidence.

Measurements of S-waves and P-waves are made at 2.5 meter intervals by lowering a single three-component geophone into the borehole and clamping it to the casing with an electrically actuated lever arm. A second three-component geophone is placed at the surface approximately 10 centimeters from the shear source and is used to check the triggering of the recorder for zero time.

P-waves are made by striking a steel plate with a sledge hammer. The steel plate is located at the surface with the same offset as the S-wave source. The recorder is triggered by the sledge hammer making electrical contact with the steel plate.

The data are recorded on magnetic tape cassettes in digital form on a twelve-channel recording system.

---

\* In this report shear-wave(s) and S-wave are used interchangeably as well as P-wave and compressional-wave.

## VELOCITY DETERMINATIONS

The flow-chart, Figure 2, describes the processing and interpretation procedures. The magnetic tape cassette contains 18 recorded traces from each depth. These include data from the surface three-component geophone and the downhole three-component geophone, a total of 6 traces for each source type (positive horizontal, negative horizontal, and vertical). As mentioned previously, the surface geophone is used only to check timing.

The orientation of the downhole geophone cannot be controlled when moving from one depth to the next, so that horizontal components are not generally oriented parallel and perpendicular to the source. This causes slight phase shifts and amplitude variations. This can have a small effect on the phase timing that is done by eye. To minimize these effects, when timing shear-wave arrivals, the horizontal components are combined (rotated to maximum) to obtain a single component of motion. The direction of motion is determined by maximizing the integral square amplitude within a time interval containing the shear wave (Boatwright et al., 1986). Rotated traces are plotted on a 20-inch computer monitor and the first shear-wave arrival is timed for each of the horizontal rotated traces. Two arrival times are obtained from picks of positive and negative shear-wave arrivals. Timing of the arrivals is done to one-millisecond precision. The two time-picks are not always identical, due to interfering waves obscuring the first shear-arrival, slight phase shifts, or amplitude differences. If the time difference is greater than about 5 milliseconds a mistake in phase correlation (perhaps due to a reversed trace, noise etc.) can be suspected and a repick may be necessary. The two picks are averaged for velocity determinations. On clear traces one-millisecond picking accuracy can be maintained; however, because of lower signal-to-noise ratios and interfering waves in the deeper sections of the boreholes, this accuracy cannot always be achieved. The arrivals are weighted by the inverse of an assigned normalized variance. A normalized standard deviation of 1 was assigned to the accurate picks and values ranging up to 5 were assigned to the others.

For determining the final velocity model there are a number of ways to proceed. In our earlier work ( e.g., Gibbs et al., 1975) we determined the initial layer boundaries from the travel-time plots by eye and then added or subtracted layers based on geologic boundaries consistent with the data. We also required at least three data points in each

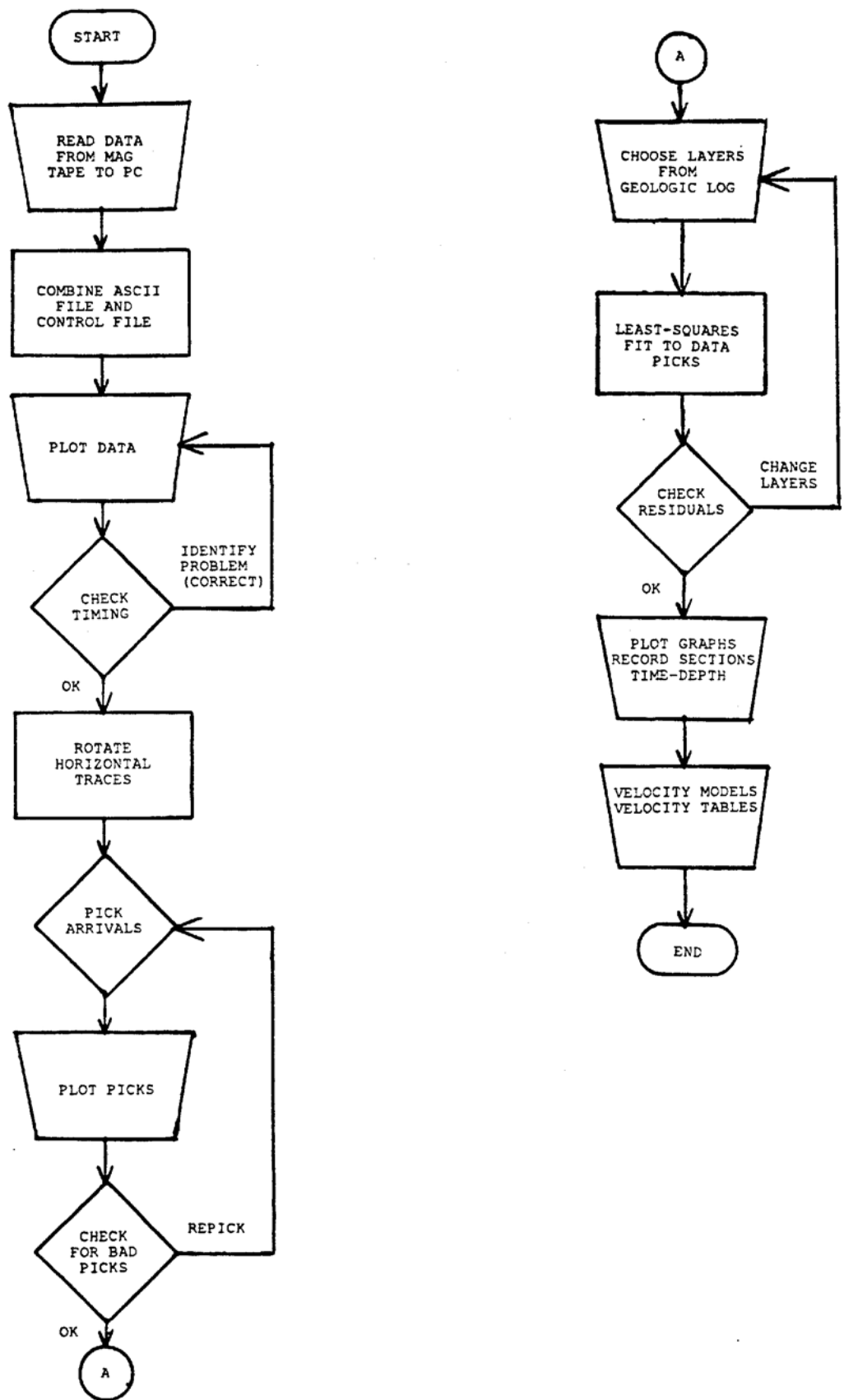


Figure 2. Flow-chart outlining the data processing and interpretation steps.

layer. This requirement limited the velocity determination to layers greater than 7.5 meters in thickness. The problem with this procedure is that a mismatch (overlap or underlap) of the line segments sometimes occurred at the intersections of the layers, resulting in a discontinuous travel-time curve. To address this problem we are now using a least-squares program LFIT (Press et al., 1992) that fits the travel-time data with line segments hinged at each selected layer boundary from the surface (forced through zero) to the bottom data point. Initial layer boundaries are chosen from the geologic log and are adjusted, if necessary, to reduce residuals and for consistency with the data (Gibbs et al., 1992). The S-wave travel-time data are analyzed first; layer boundaries are initially the same for the P-wave model, and are then adjusted, if necessary, by adding a layer for the water table or reducing the number of layers. The velocity plots (e.g. Figure A-4a) show upper and lower bounds that approximate 68% confidence limits. These bounds are not symmetrical because they are based on the standard deviation of the slope of the least-squares line fit to the travel-time plots (the inverse of the velocity).

## RESULTS

### Lithologic Logs

The lithology at Bessie Carmichael School, as determined from drill cuttings, is 7 meters of fill underlain by a 25 meter thick section of soft Bay Mud (see Figure A-1). The mud section grades to clay and sandy clay in the bottom 10 meters. Below this is a 20 meter layer of sand (Colma fm.?) underlain by 20 meters of stiff to hard clay (Older Bay Mud). Bedrock is encountered at 74 meters (serpentine) and Franciscan shale at 82 meters. The borehole bottoms in shale at 90 meters.

Embarcadero Plaza lithology is 8.5 meters of fill overlying 25 meters of Holocene Bay Mud (see Figure B-1). A sand layer 10 meters thick lies beneath the mud and a 20 meter thick section of Older Bay Mud overlies a thin layer of bedrock (Franciscan Greywacke) at a depth of 65 meters. Sandstone is encountered at a depth of 66 meters and the hole bottoms in this formation at 77 meters.

At Levi Plaza 6 meters of fill overlie 14 meters of Holocene Bay Mud (see Figure C-1). Below the mud lies 9 meters of mostly sand with thin clay layers and bedrock (shale) is encountered at 29 meters. The borehole bottoms at 42 meters still in shale.

In brief, the three sites have similar lithology (fill - bay mud - sand - older bay mud - bedrock) with the Older Bay Mud layer missing at Levi Plaza.

### **S-wave Velocities**

Shear-wave velocities obtained at the three sites are summarized in Figure 3. Velocities obtained for artificial fill from previous studies ranged from 135 to 250 meters/second (m/s). The fill-velocities from these sites are: 250 m/s at Bessie Carmichael School, 290 m/s at Embarcadero Plaza, and 360 m/s at Levi Plaza. These fill-velocities are somewhat higher than obtained from earlier results and may be due to better mechanical compaction. The average S-wave velocities through the Bay Mud sections are: 129 m/s at Bessie Carmichael School, 130 m/s at Embarcadero Plaza, and 121 m/s at Levi Plaza. The low-velocity mud-sections control the character of earthquake ground-motions at these sites. The average velocities to a depth of 30 meters are: 171 m/s at Bessie Carmichael School, 167 m/s at Embarcadero Plaza, and 197 m/s at Levi Plaza. Average velocity to other borehole depths can be calculated using the tables located in the appendices.

### **P-wave Velocities**

Figure 4 summarizes compressional-wave velocities of the three sites. There is a poorer correlation between P-wave velocity and lithology, than S-wave velocity and lithology because P-wave velocity is strongly affected by degree of saturation. Note that even though the Holocene Bay Mud is saturated, the P-wave velocities measured are less than the velocity of P-waves in water ( $\approx 1500$  meters/second). The explanation for this may be that gas is trapped in the mud as pointed out by Brandt, 1960 (e.g. methane from decaying organic matter). Average P-wave velocities in the Bay Mud are: 780 m/s at Bessie Carmichael School, 790 m/s at Embarcadero Plaza, and 800 m/s at Levi Plaza. Corresponding average velocities to 30 meters depth are 880 m/s, 910 m/s, and 1010 m/s, respectively.

Detailed geologic and seismic results are provided in Appendix-A for Bessie Carmichael School, Appendix-B for Embarcadero Plaza and Appendix-C for Levi Plaza. The appendices include geologic logs, record sections, travel-time graphs, P- and S-wave velocity models, and data tables for each site.

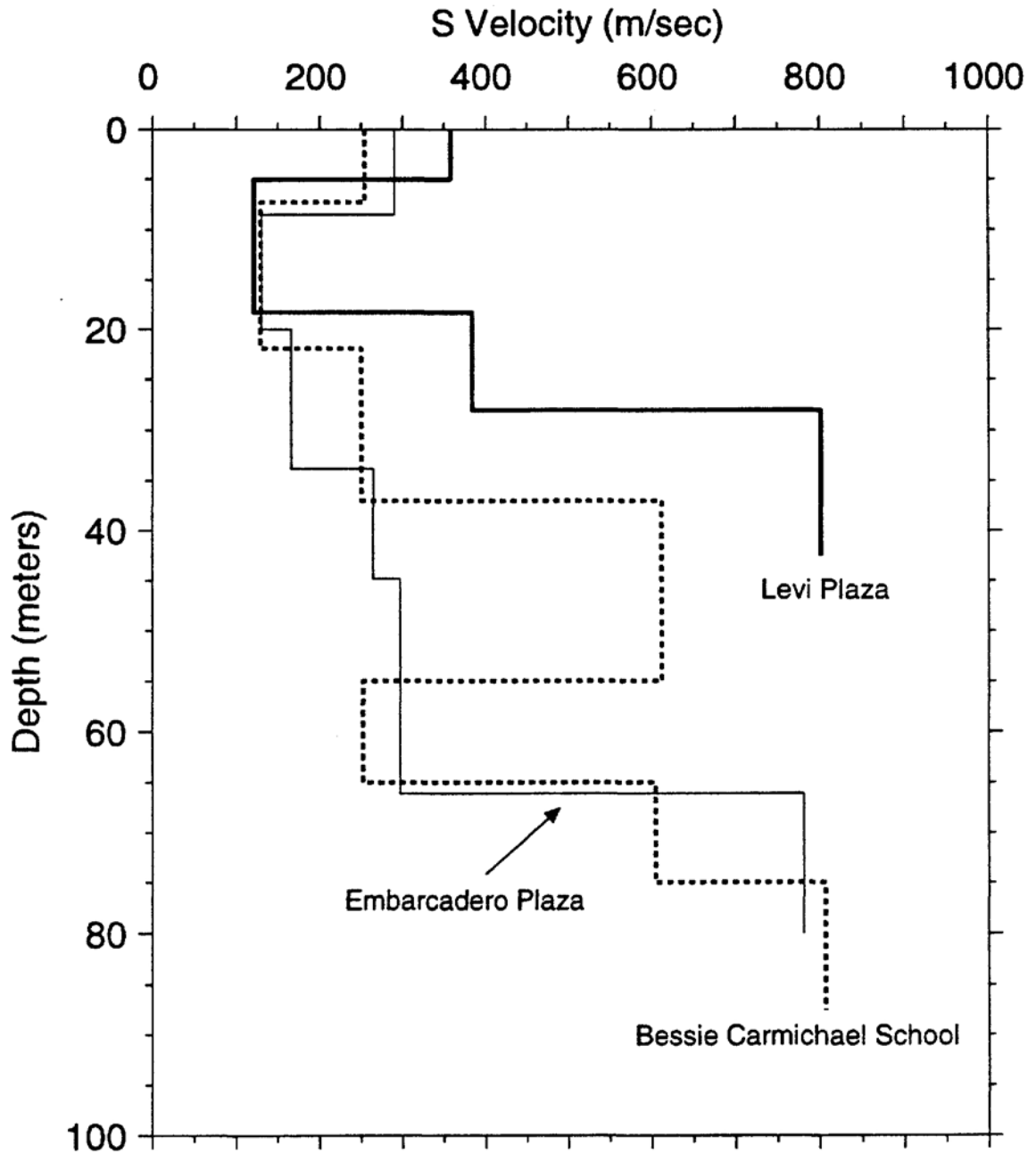


Figure 3. S-wave velocity models superimposed for comparison. The three sites shown have Holocene Bay Mud deposits near the surface overlain by varied thicknesses of artificial fill.

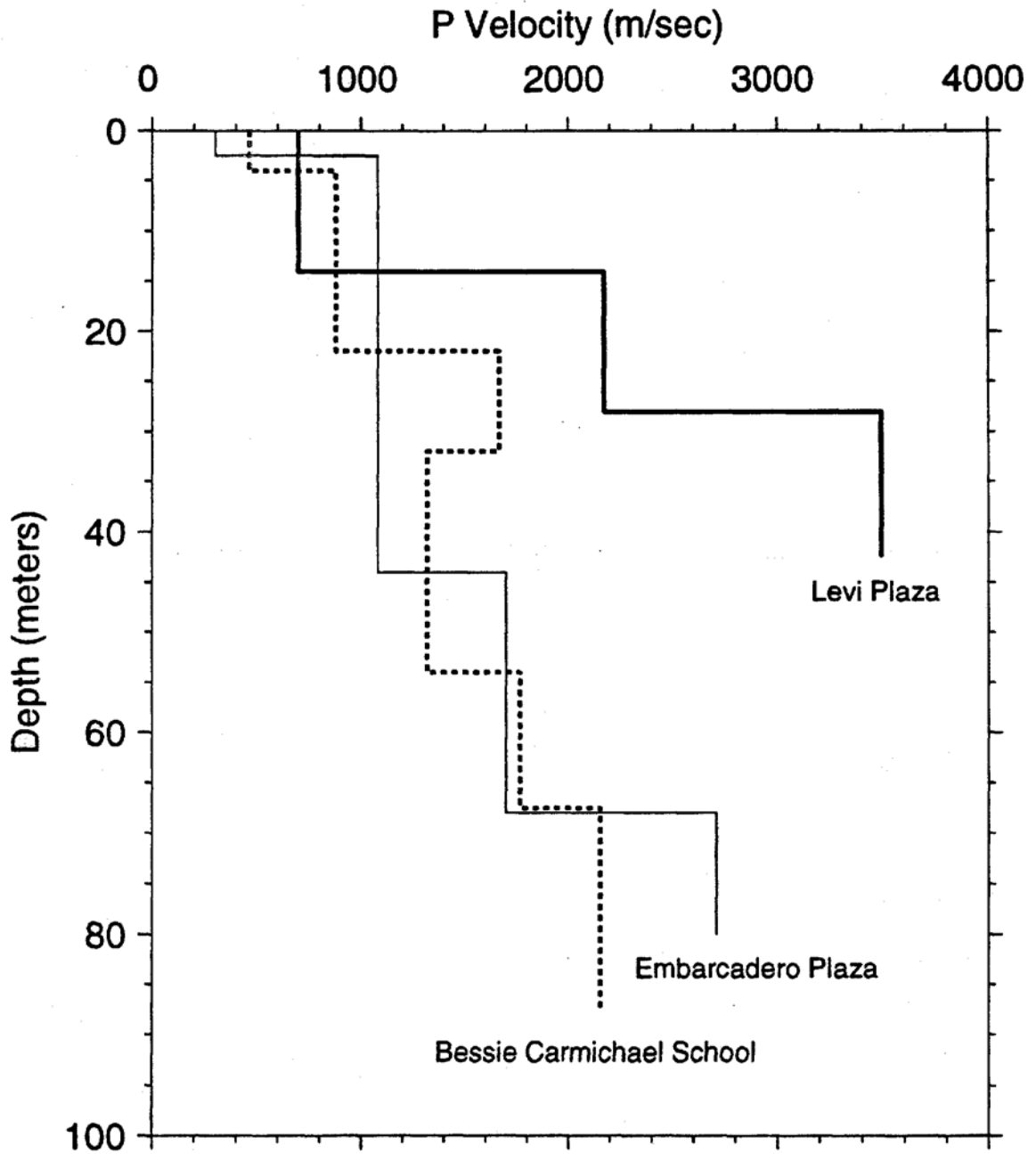


Figure 4. P-wave velocity models superimposed for comparison.

## ACKNOWLEDGMENTS

The authors and the U.S. Geological Survey would like to thank: Mr. Michael D. Franklin, Property Manager, Interland and Jalson; Mr. Cliff Jarrard, Chief Harbor Engineer; Mr. Ed Bubnis, Chief Inspector, Port of San Francisco; for their help in obtaining permission to install earthquake monitoring instruments at the Levi Plaza site: Mr. Jon Huttinger, Superintendent of Parks, San Francisco Parks and Recreation Department, for permission at the Embarcadero Plaza site: Mr. Thomas Sammon, Executive Assistant to the Superintendent, San Francisco Unified School District and Mrs. Amy Talisman, Principal, for permission at the Bessie Charmichael School site. We also wish to thank Mr. Dick Lake, CEO and Mr. Roger Kostenko, Driller, of the Pitcher Drilling Company.

## REFERENCES

- Boatwright, John, R. Porcella, T. Fumal, and Hsi-Ping Liu, 1986, Direct estimates of shear wave amplification and attenuation from a borehole near Coalinga, California: *Earthquake Notes*, v. 57, p. 8.
- Borcherdt, R. D., 1970, Effects of local geology on ground motion near San Francisco Bay: *Bull. Seismo. Soc. Am.* v. 60, pp. 29-61.
- Borcherdt, Roger D., and James F. Gibbs, 1976, Effects of local geological conditions in the San Francisco Bay region on ground motions and the intensities of the 1906 earthquake: *Bull. Seismo. Soc. Am.* v. 66, pp. 467-500.
- Borcherdt, Roger D., and Gary Glassmoyer, 1992, On the characteristics of local geology and their influence on ground motions generated by the Loma Prieta earthquake in the San Francisco Bay Region, California: *Bull. Seismo. Soc. Am.* v. 82, pp. 603-641.
- Brandt, H., 1960, Factors affecting compressional wave velocity in unconsolidated marine sediments: *Acoustical Soc. Am. Jour.*, v. 32, pp. 171-179.
- Ellen, S. D., C. M. Wentworth, E. E. Brabb, and E. H. Pampeyan, 1972, Description of geologic units, San Mateo County, California: Accompanying U.S. Geological Survey Miscellaneous Field Studies Map, MF-328.
- Gibbs, James F., Thomas E. Fumal, David M. Boore, and William B. Joyner, 1992, Seismic velocities and geologic logs from borehole measurements at seven strong-motion stations that recorded the Loma Prieta earthquake: U.S. Geological Survey, Open-File Report 92-287.
- Gibbs, James F., Thomas E. Fumal, and Roger D. Borcherdt, 1975, In-situ measurements of seismic velocities at twelve locations in the San Francisco Bay region: U.S. Geological Survey, Open-file report 75-564, 87p.
- Lawson, A. C., (chairman), 1908, The California earthquake of April 18, 1906: Report of the State Earthquake Commission, Carnegie Inst. Washington.
- Liu, Hsi-Ping, Richard E. Warrick, Robert E. Westerlund, Jon B. Fletcher, and Gary L. Maxwell, 1988, An air-powered impulsive shear-wave source with repeatable signals: *Bull. Seismo. Soc. Am.*, v. 78, p.355-369.
- Press, William H., Brian P. Flannery, Saul A. Teukolsky, and William T. Vetterling, 1992, *Numerical Recipes, the art of scientific computing, General Linear Least Squares*: Cambridge University Press, Cambridge, p. 665-670.
- Soil Survey Staff, 1951, U.S. Department of Agriculture Handbook 18: U.S. Government Printing Office, Washington D.C. 20402, 503p.
- Terzaghi, Karl, and Ralph B. Peck, 1967, *Soil mechanics in engineering practice*: John Wiley and Sons, New York, 2nd edition.

**Definitions of terms used for descriptions of sedimentary deposits and bedrock materials**

**Rock hardness:** response to hand and geologic hammer: (Ellen et al., 1972)

- hard - hammer bounces off with solid sound
- firm - hammer dents with thud, pick point dents or penetrates slightly
- soft - pick points penetrates
- friable material can be crumbled into individual grains by hand.

**Fracture spacing:** (Ellen et al., 1972)

cm	in	fracture spacing
0-1	0-1/2	v. close
1-5	1/2-2	close
5-30	2-12	moderate
30-100	12-36	wide
> 100	> 36	v. wide

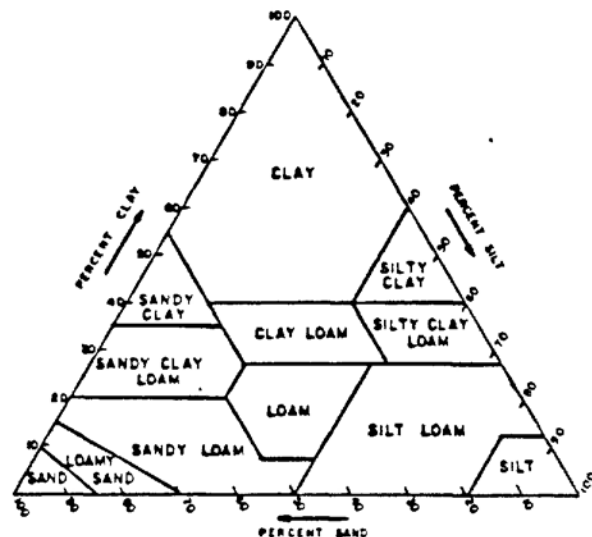
**Weathering:**

- Fresh: no visible signs of weathering
- Slight: no visible decomposition of minerals, slight discoloration
- Moderate: slight decomposition of minerals and disintegration of rock, deep and thorough discoloration
- Deep: extensive decomposition of minerals and complete disintegration of rock but original structure is preserved.

Relative density of sand and consistency of clay is correlated with penetration resistance: (Terzaghi and Peck, 1948)

blows/ft.	relative density	blows/ft.	consistency
0-4	v. loose	< 2	v. soft
4-10	loose	2-4	soft
10-30	medium	4-8	medium
30-50	dense	8-15	stiff
> 50	v. dense	15-30	v. stiff
		> 30	hard

**Texture:** the relative proportions of clay, silt, and sand below 2mm. Proportions of larger particles are indicated by modifiers of textural class names. Determination is made in the field mainly by feeling the moist soil (Soil Survey, Staff, 1951).



**Color:** Standard Munsell color names are given for the dominant color of the moist soil and for prominent mottles.

**Types of samples**

- SP - Standard Penetration 1 + 3/8 in in ID sampler)
- S - Thin-wall push sampler
- O - Osterberg fixed-piston sampler
- P - Pitcher Barrel sampler
- CH - California Penetration (2 in ID sampler)
- DC - Diamond Core

Figure 5. Explanation of geologic logs.



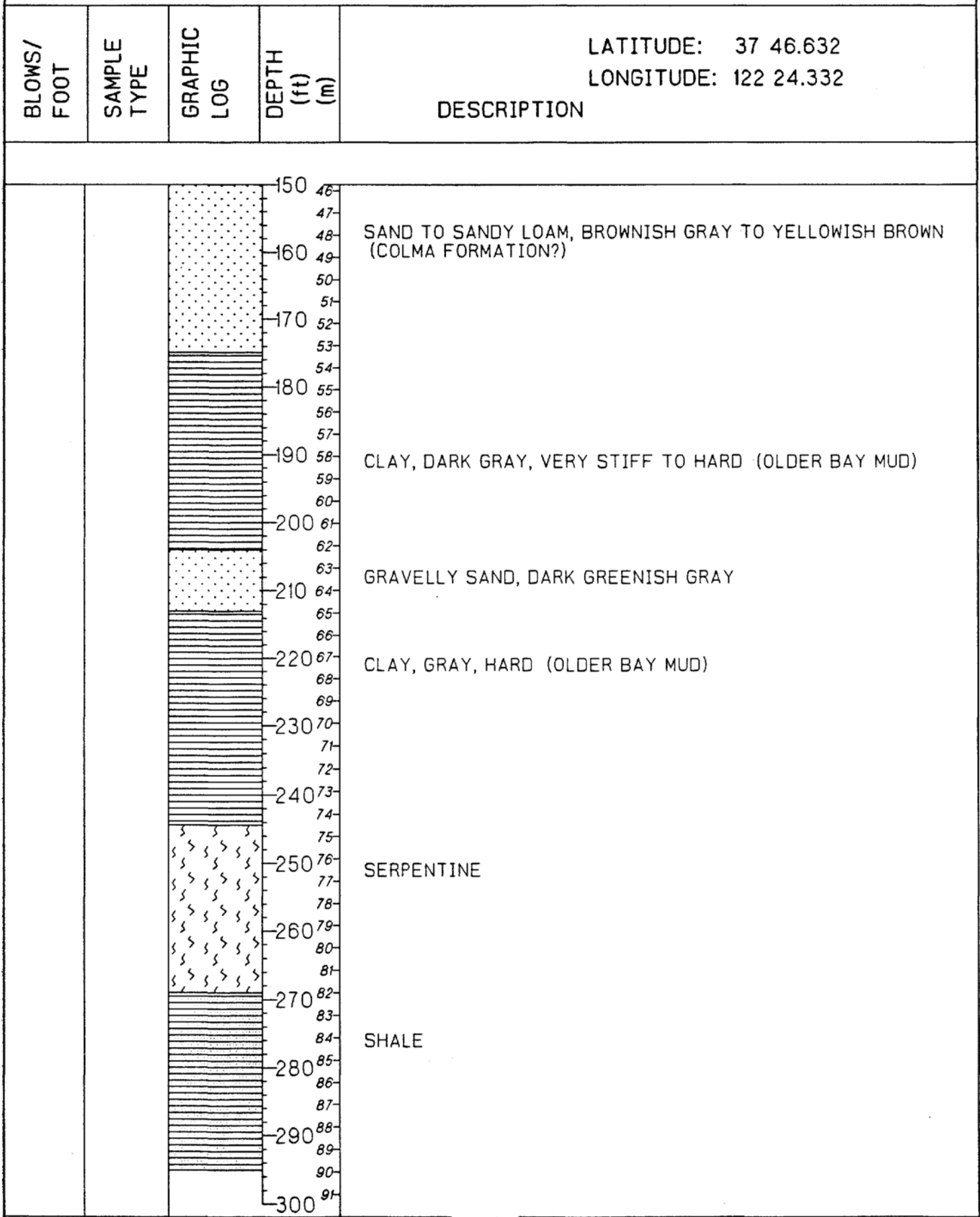
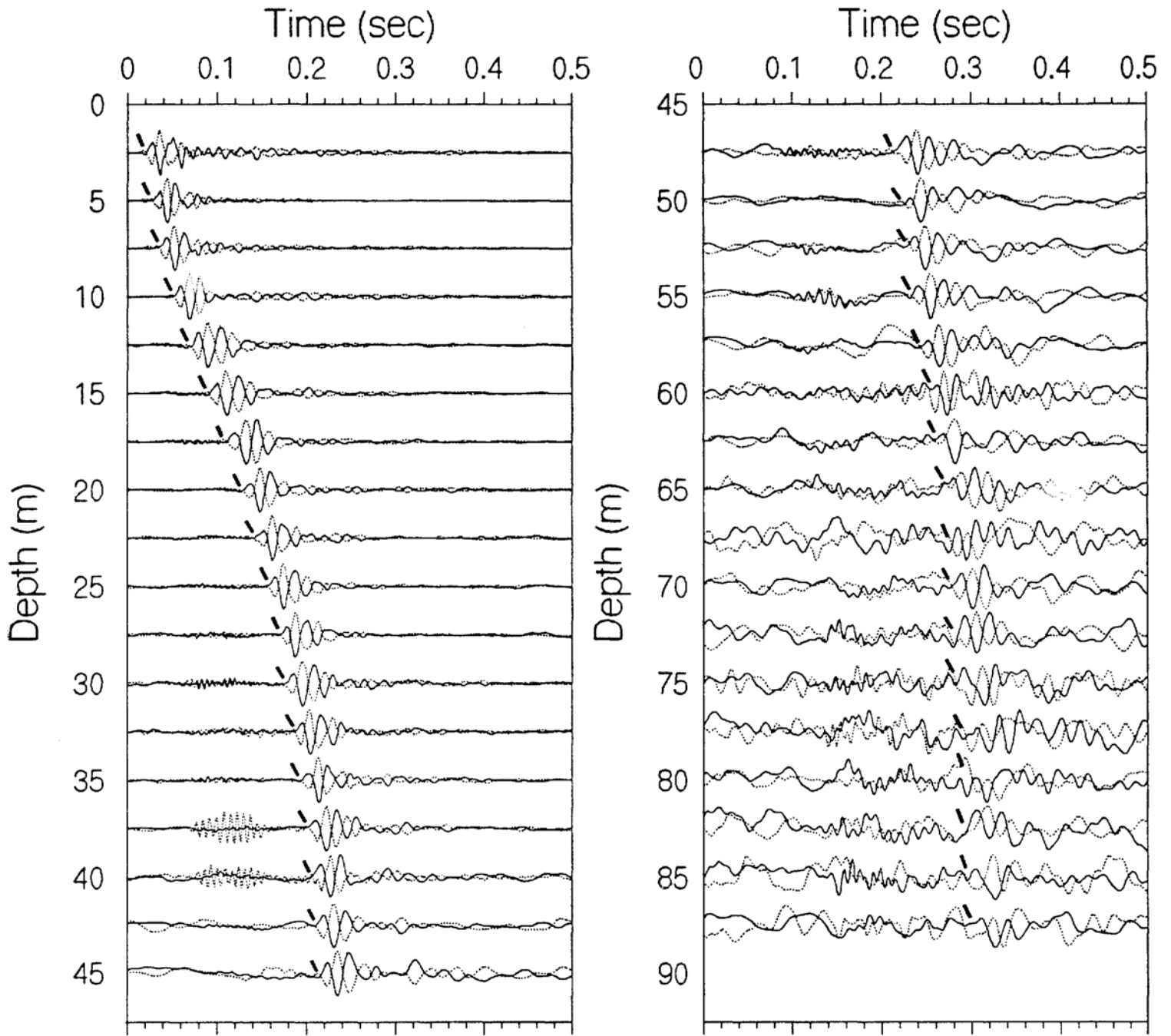
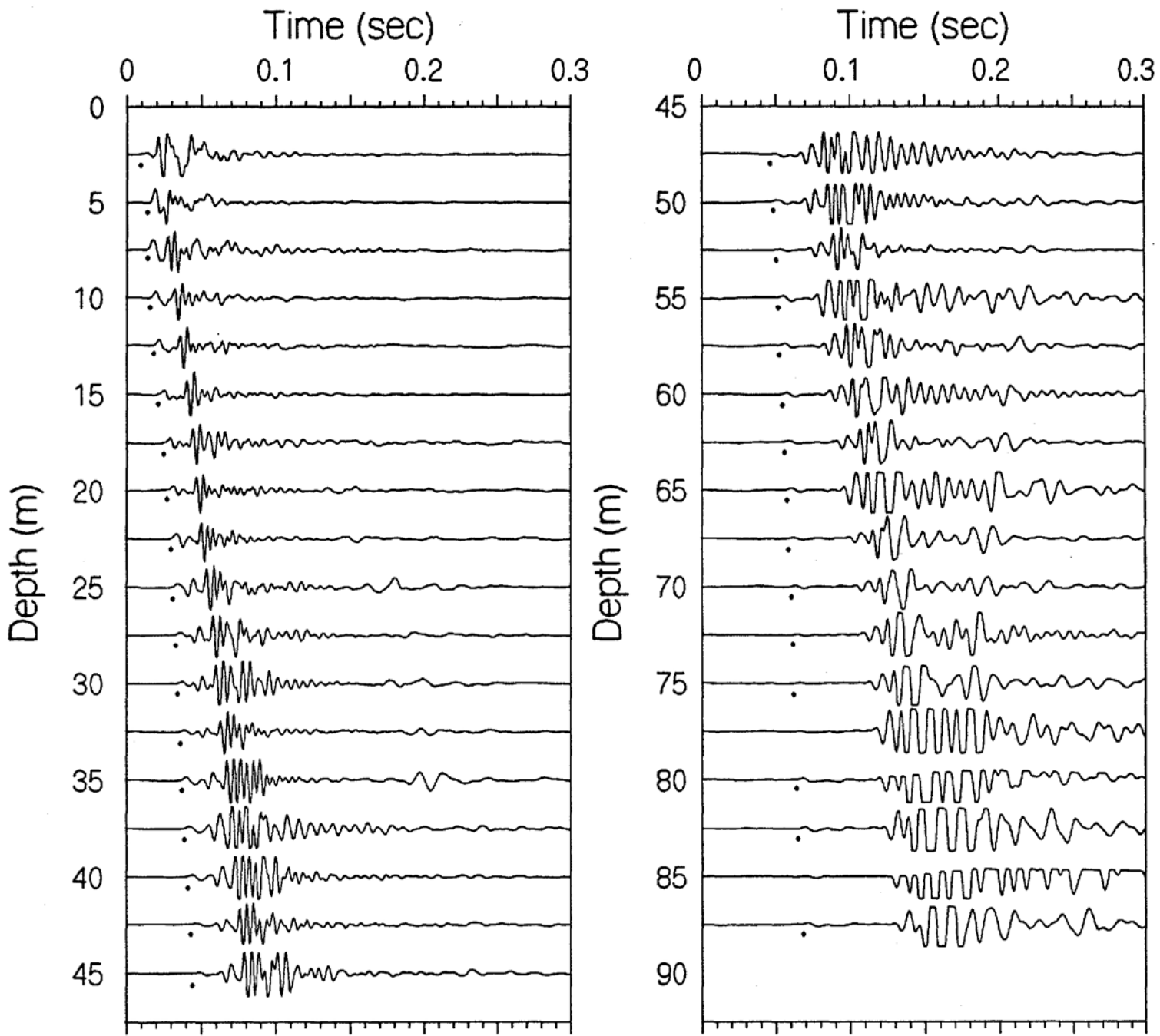


Figure A1. (Continued).



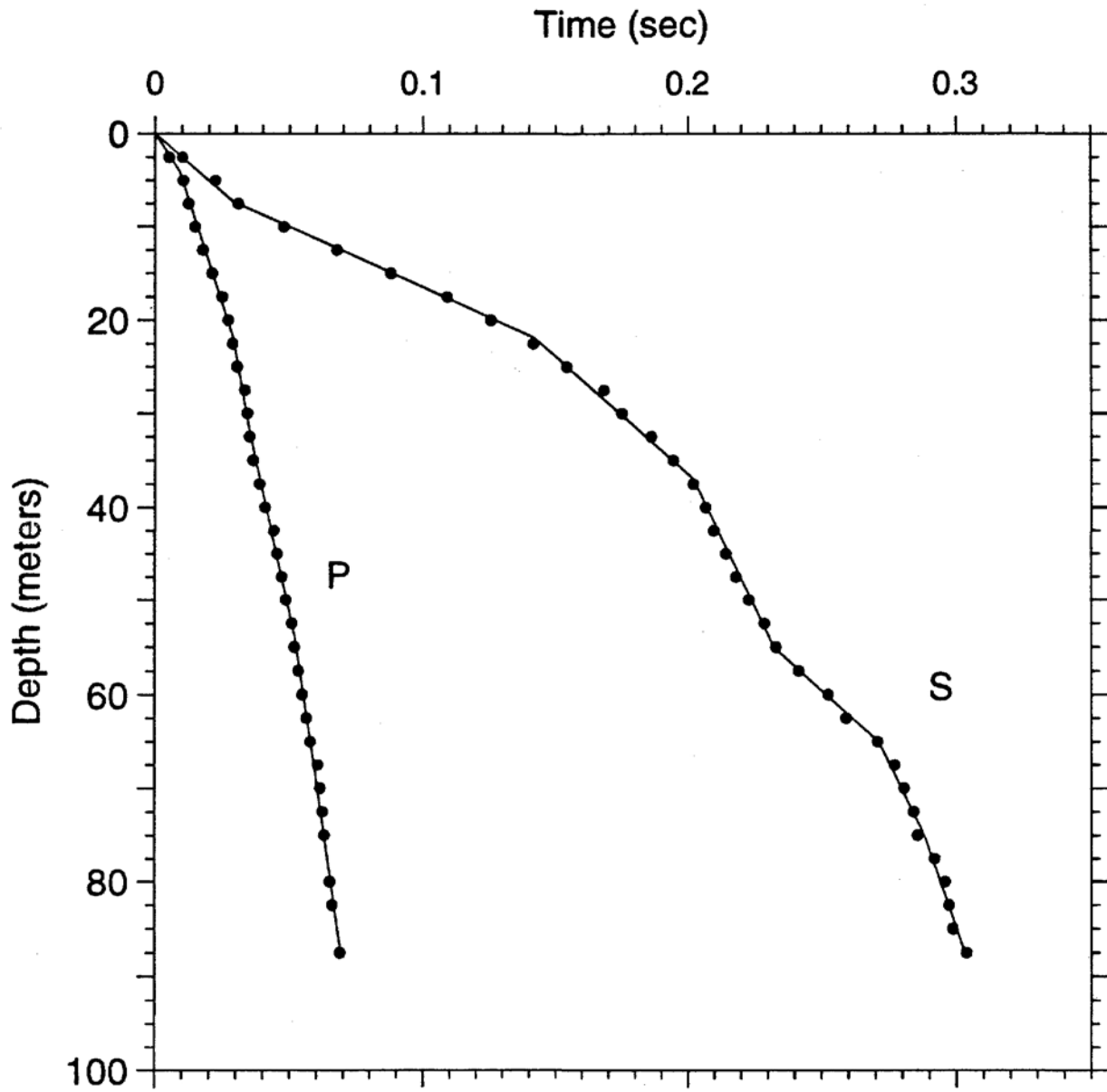
### Bessie Carmichael School

Figure A2a. Record section of impacts from opposite horizontal directions superimposed for identification of S-wave onset. Approximate S-wave picks are shown by the accent marks.



### Bessie Carmichael School

Figure A2b. Vertical-component record section. P-wave arrivals are shown by the solid circles.



Bessie Carmichael School

Figure A3. Time-depth graph of P-wave and S-wave picks. Line segments show the hinged-least-squares fit to the data points.

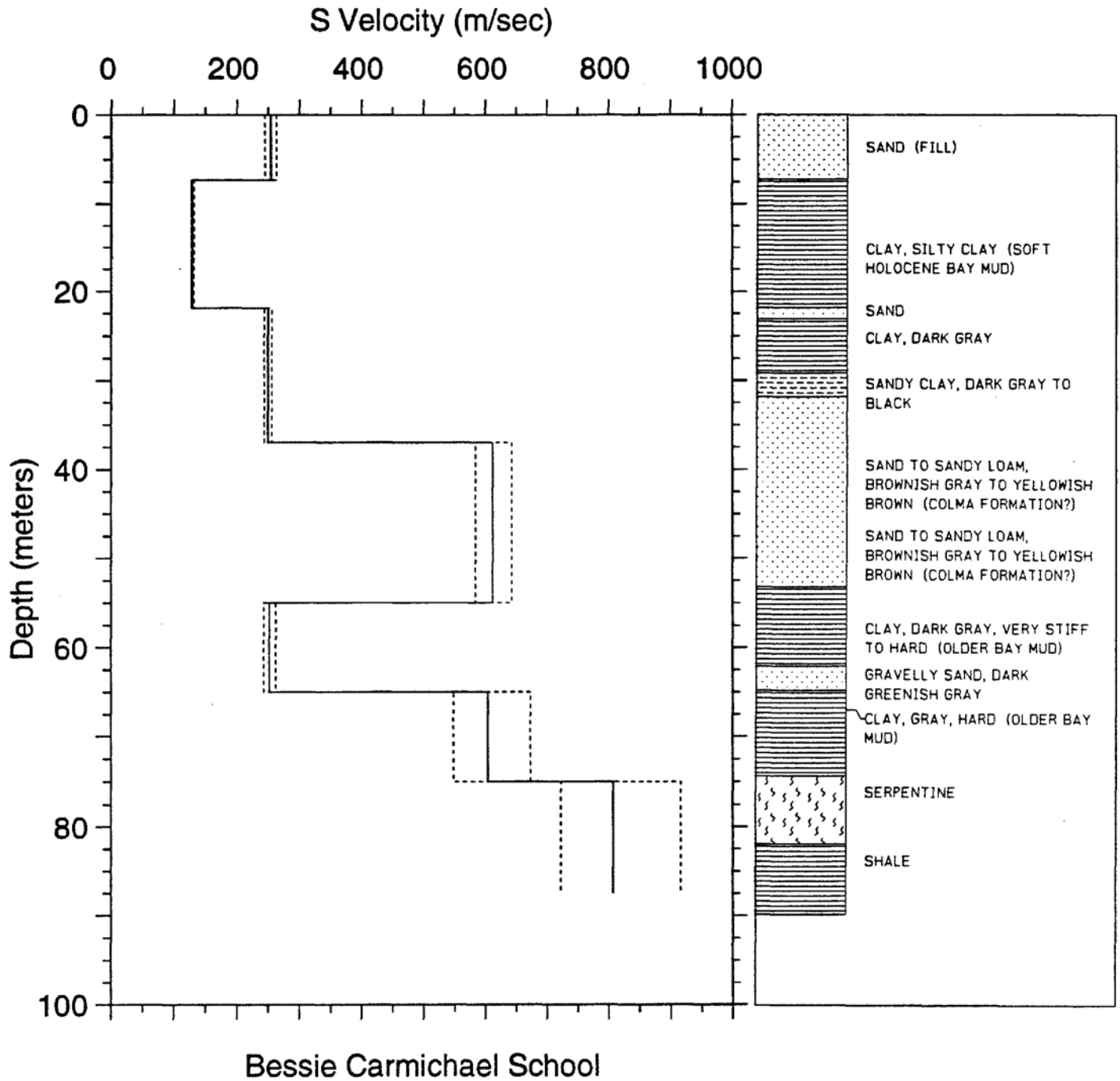


Figure A4a. S-wave velocity profiles with dashed lines representing plus and minus one standard deviation. Simplified geologic log is shown for correlation with velocities.

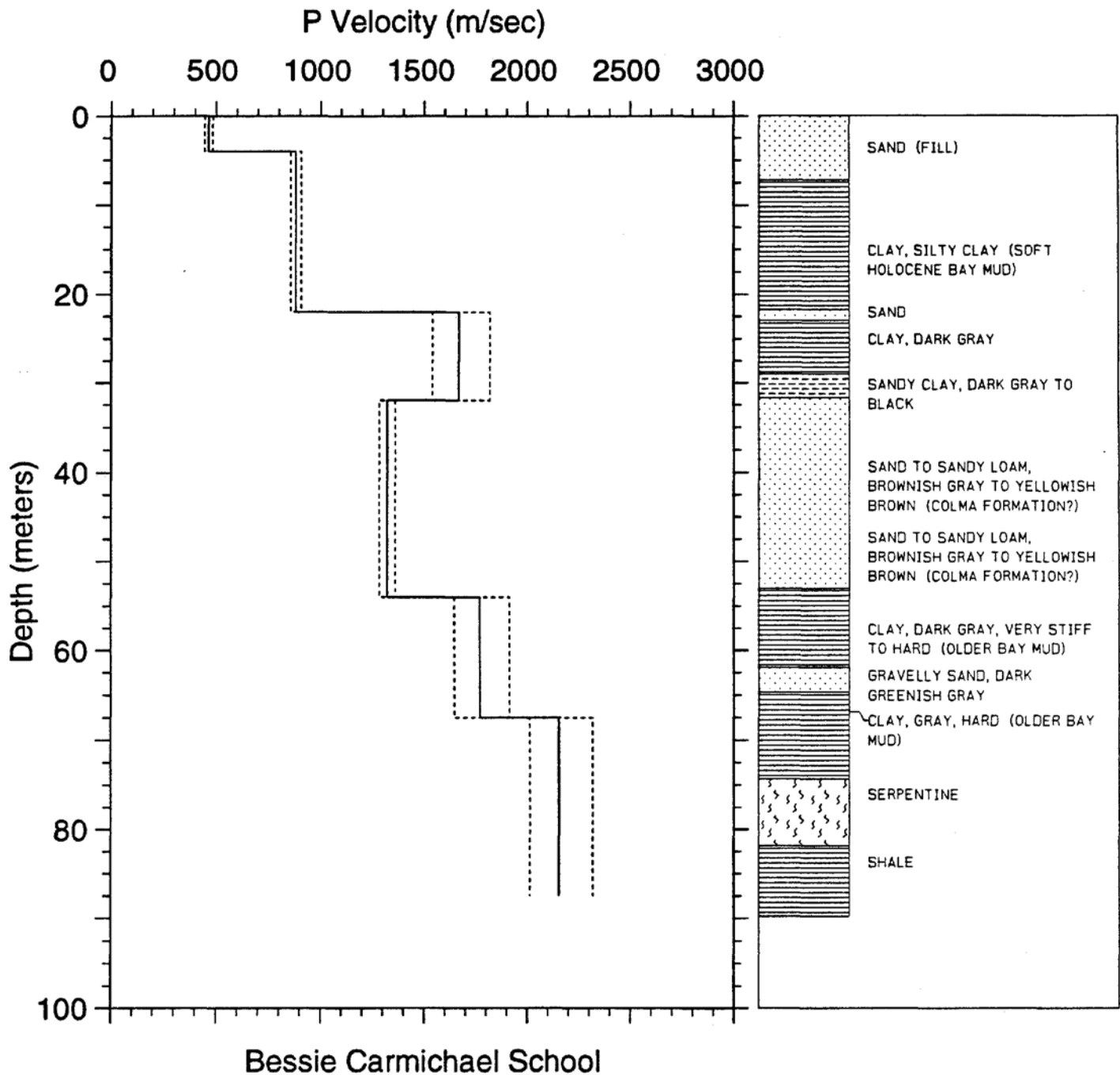


Figure A4b. P-wave velocity profiles with dashed lines representing plus and minus one standard deviation. Simplified geologic log is shown for correlation with velocities.

TABLE A1a. S-wave arrival times and velocity summaries for Bessie Carmichael School.

d(m)	d(ft)	t(sec)	sig	rsdl/sig	dtb(m)	dtb(ft)	ttb(s)	v(m/s)	vl(m/s)	vu(m/s)	v(ft/s)	vl(ft/s)	vu(ft/s)
2.5	8.2	.0101	1	.2	.0	.0	.000						
5.0	16.4	.0223	1	2.6	7.3	24.0	.029	254	245	263	832	804	862
7.5	24.6	.0309	1	.6	21.9	71.9	.142	129	128	131	424	419	430
10.0	32.8	.0478	1	-1.9	37.0	121.4	.202	250	244	256	819	801	839
12.5	41.0	.0676	1	-1.4	55.0	180.4	.232	612	584	643	2007	1915	2108
15.0	49.2	.0879	1	-.4	65.0	213.3	.271	252	243	262	827	796	859
17.5	57.4	.1090	1	1.4	75.0	246.1	.288	604	548	673	1981	1796	2208
20.0	65.6	.1255	1	-1.5	87.5	287.1	.303	807	722	916	2649	2368	3005
22.5	73.8	.1416	1	-2.5									
25.0	82.0	.1542	1	.1									
27.5	90.2	.1682	1	4.1									
30.0	98.4	.1750	1	-.9									
32.5	106.6	.1861	1	2.0									
35.0	114.8	.1944	1	-.3									
37.5	123.0	.2019	1	-1.0									
40.0	131.2	.2065	1	-.5									
42.5	139.4	.2096	1	-1.5									
45.0	147.6	.2142	1	-1.0									
47.5	155.8	.2180	1	-1.3									
50.0	164.0	.2228	1	-.6									
52.5	172.2	.2286	1	1.1									
55.0	180.4	.2329	1	1.3									
57.5	188.6	.2414	1	-.1									
60.0	196.9	.2524	1	1.0									
62.5	205.1	.2590	1	-2.3									
65.0	213.3	.2707	1	-.5									
67.5	221.5	.2770	1	1.6									
70.0	229.7	.2805	1	1.0									
72.5	237.9	.2841	1	.4									
75.0	246.1	.2856	1	-2.2									
77.5	254.3	.2919	2	.5									
80.0	262.5	.2958	1	1.8									
82.5	270.7	.2972	2	-.1									
85.0	278.9	.2987	1	-1.5									
87.5	287.1	.3037	1	.4									

Explanation:

d(m) = depth in meters

d(ft) = depth in feet

t(sec) = arrival time in seconds (S-wave arrival times are the average of picks from traces obtained from hammer blows differing in direction by 180°)

sig = sigma, standard deviation normalized to the standard deviation of best picks

rsdl/sig = least-squares residual divided by sigma

dtb(m) = depth to bottom of layer in meters

dtb(ft) = depth to bottom of layer in feet

ttb(s) = arrival time in seconds to bottom of layer

v(m/s) = velocity in meters per second

vl(m/s) = lower limit of velocity in meters per second \*

vu(m/s) = upper limit of velocity in meters per second

v(ft/s) = velocity in feet per second

vl(ft/s) = lower limit of velocity in feet per second

vu(ft/s) = upper limit of velocity in feet per second

\* see text for explanation of velocity limits

TABLE A1b. P-wave arrival times and velocity summaries for Bessie Carmichael School.

d(m)	d(ft)	t(sec)	sig	rsdl/sig	dtb(m)	dtb(ft)	tth(s)	v(m/s)	vl(m/s)	vu(m/s)	v(ft/s)	vl(ft/s)	vu(ft/s)
2.5	8.2	.0052	1	-.2	.0	.0	.000						
5.0	16.4	.0105	1	.7	4.0	13.1	.009	464	446	484	1523	1463	1588
7.5	24.6	.0124	1	-.2	22.0	72.2	.029	881	856	907	2890	2810	2975
10.0	32.8	.0148	1	-.6	32.0	105.0	.035	1667	1540	1818	5470	5052	5964
12.5	41.0	.0177	1	-.6	54.0	177.2	.052	1321	1284	1360	4335	4214	4463
15.0	49.2	.0212	1	-.1	67.5	221.5	.059	1770	1646	1914	5807	5401	6279
17.5	57.4	.0249	1	1.0	87.5	287.1	.069	2155	2014	2318	7071	6608	7605
20.0	65.6	.0271	2	.2									
22.5	73.8	.0287	1	-.7									
25.0	82.0	.0305	1	-.4									
27.5	90.2	.0333	1	.9									
30.0	98.4	.0342	1	.3									
32.5	106.6	.0351	1	-.3									
35.0	114.8	.0364	1	-.9									
37.5	123.0	.0388	1	-.4									
40.0	131.2	.0409	1	-.2									
42.5	139.4	.0442	1	1.2									
45.0	147.6	.0454	1	.5									
47.5	155.8	.0472	2	.2									
50.0	164.0	.0487	1	.0									
52.5	172.2	.0509	1	.3									
55.0	180.4	.0518	1	-.5									
57.5	188.6	.0533	1	-.4									
60.0	196.9	.0548	1	-.3									
62.5	205.1	.0563	1	-.2									
65.0	213.3	.0578	1	-.1									
67.5	221.5	.0605	2	.6									
70.0	229.7	.0614	2	.5									
72.5	237.9	.0623	2	.3									
75.0	246.1	.0629	2	.0									
80.0	262.5	.0650	1	-.1									
82.5	270.7	.0659	1	-.4									
87.5	287.1	.0689	1	.3									

Explanation:

d(m) = depth in meters

d(ft) = depth in feet

t(sec) = arrival time in seconds (S-wave arrival times are the average of picks from traces obtained from hammer blows differing in direction by 180°)

sig = sigma, standard deviation normalized to the standard deviation of best picks

rsdl/sig = least-squares residual divided by sigma

dtb(m) = depth to bottom of layer in meters

dtb(ft) = depth to bottom of layer in feet

tth(s) = arrival time in seconds to bottom of layer

v(m/s) = velocity in meters per second

vl(m/s) = lower limit of velocity in meters per second \*

vu(m/s) = upper limit of velocity in meters per second

v(ft/s) = velocity in feet per second

vl(ft/s) = lower limit of velocity in feet per second

vu(ft/s) = upper limit of velocity in feet per second

\* see text for explanation of velocity limits



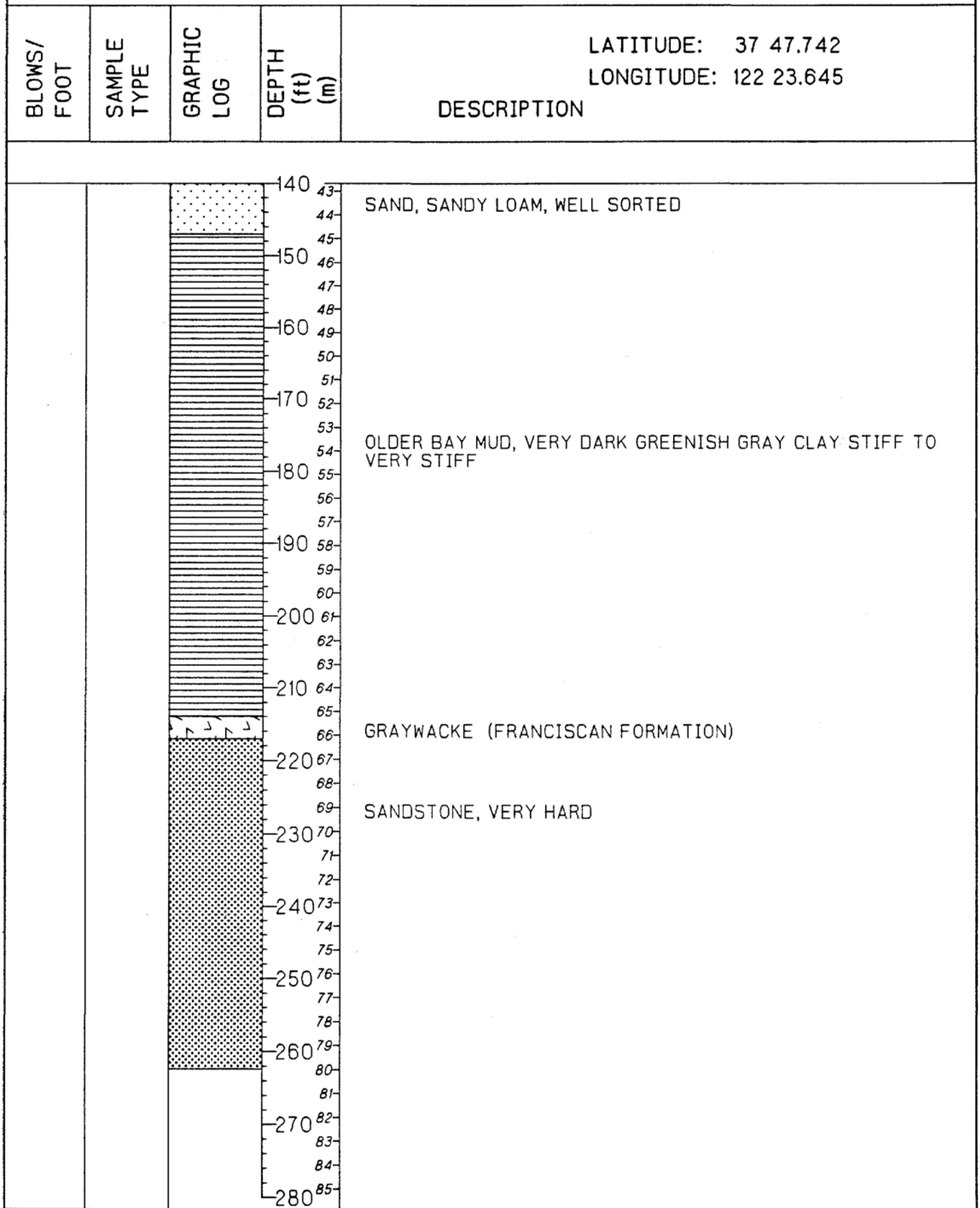
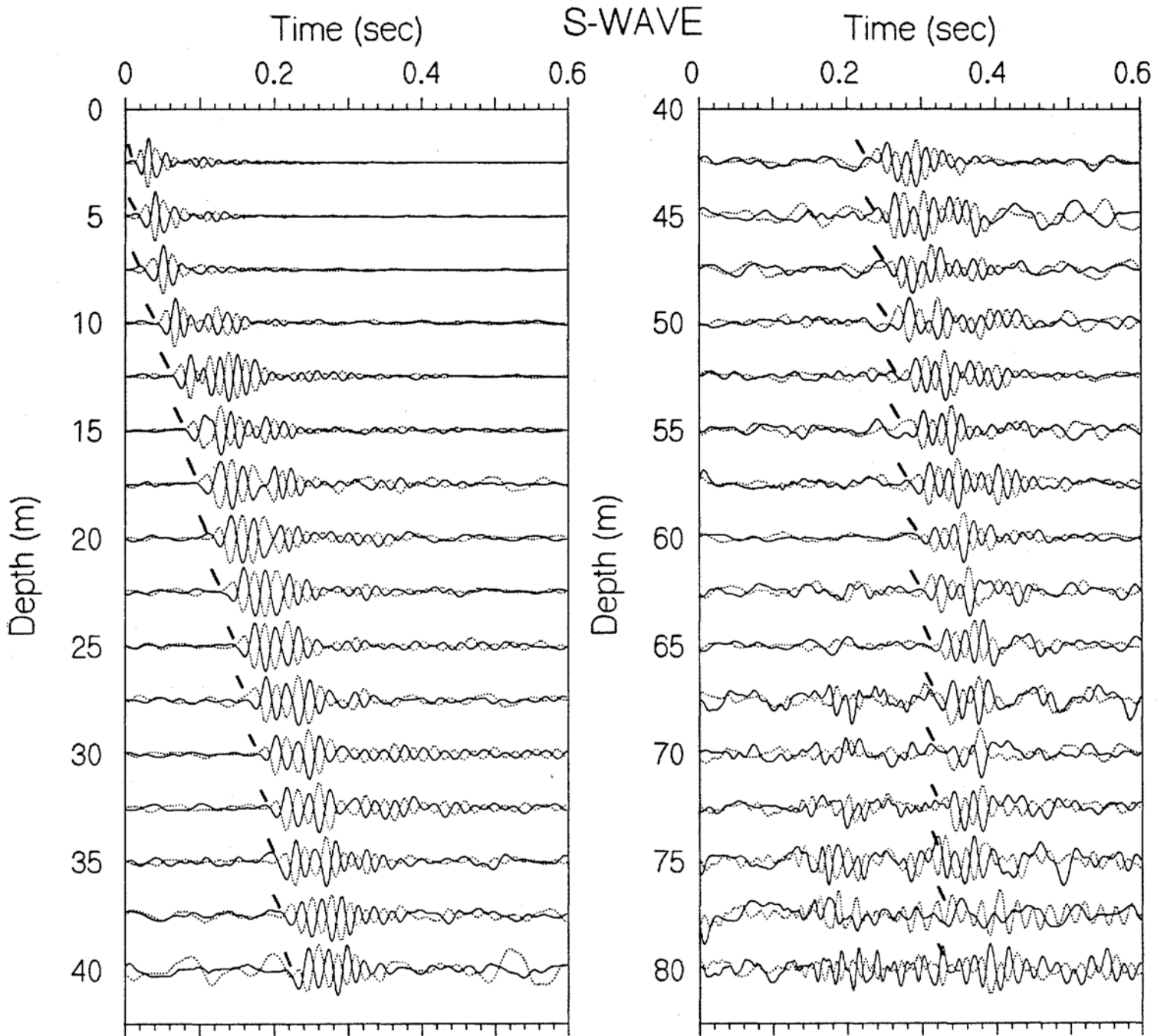
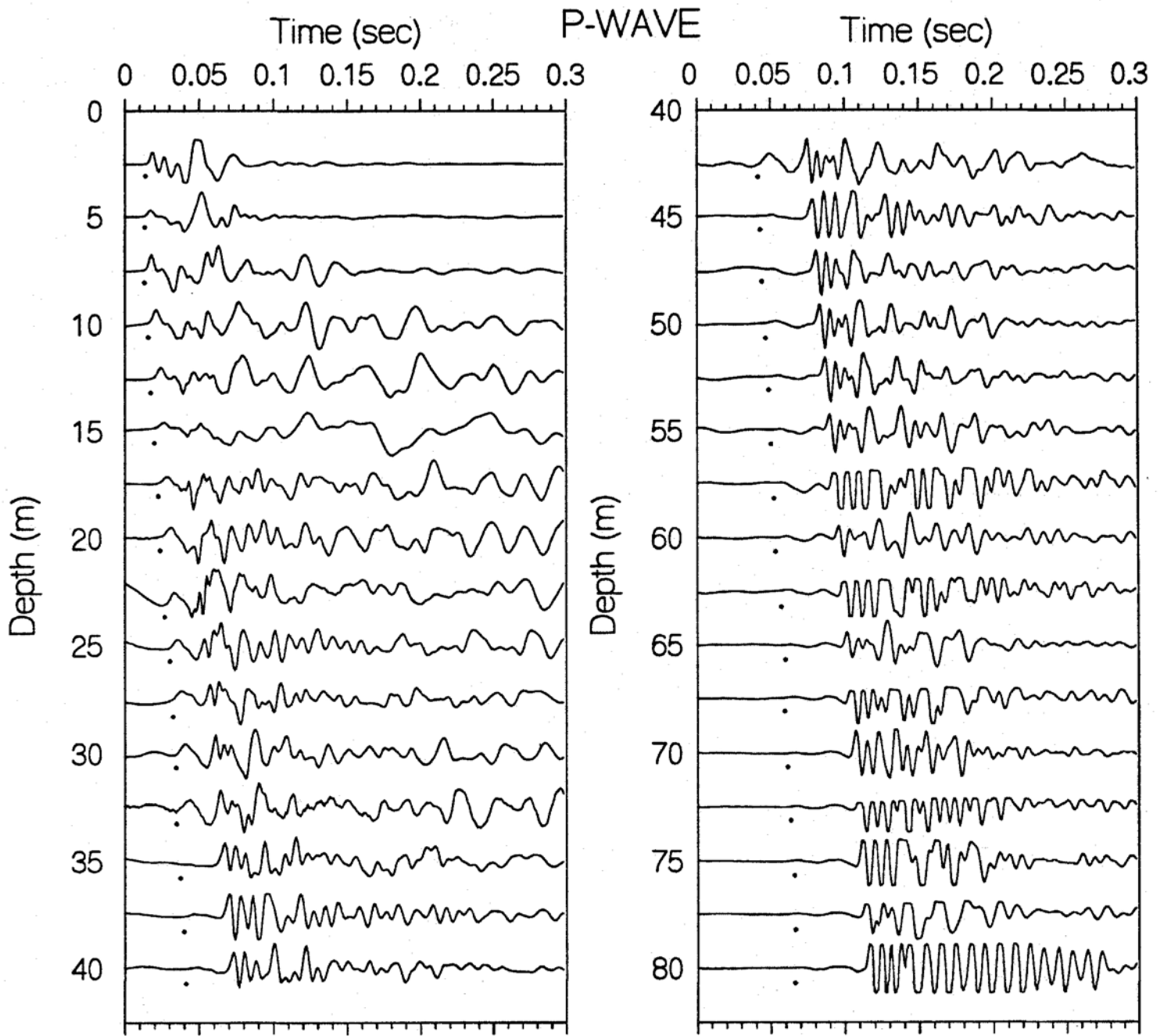


Figure B1. (Continued).



## Embarcadero

Figure B2a. Horizontal-component record section (from horizontal impacts in opposite directions) superimposed for identification of S-wave arrivals. Approximate S-wave picks are shown by the accent marks.



### Embarcadero Plaza

Figure B2b. Vertical-component record section. P-waves are shown by the solid circles.

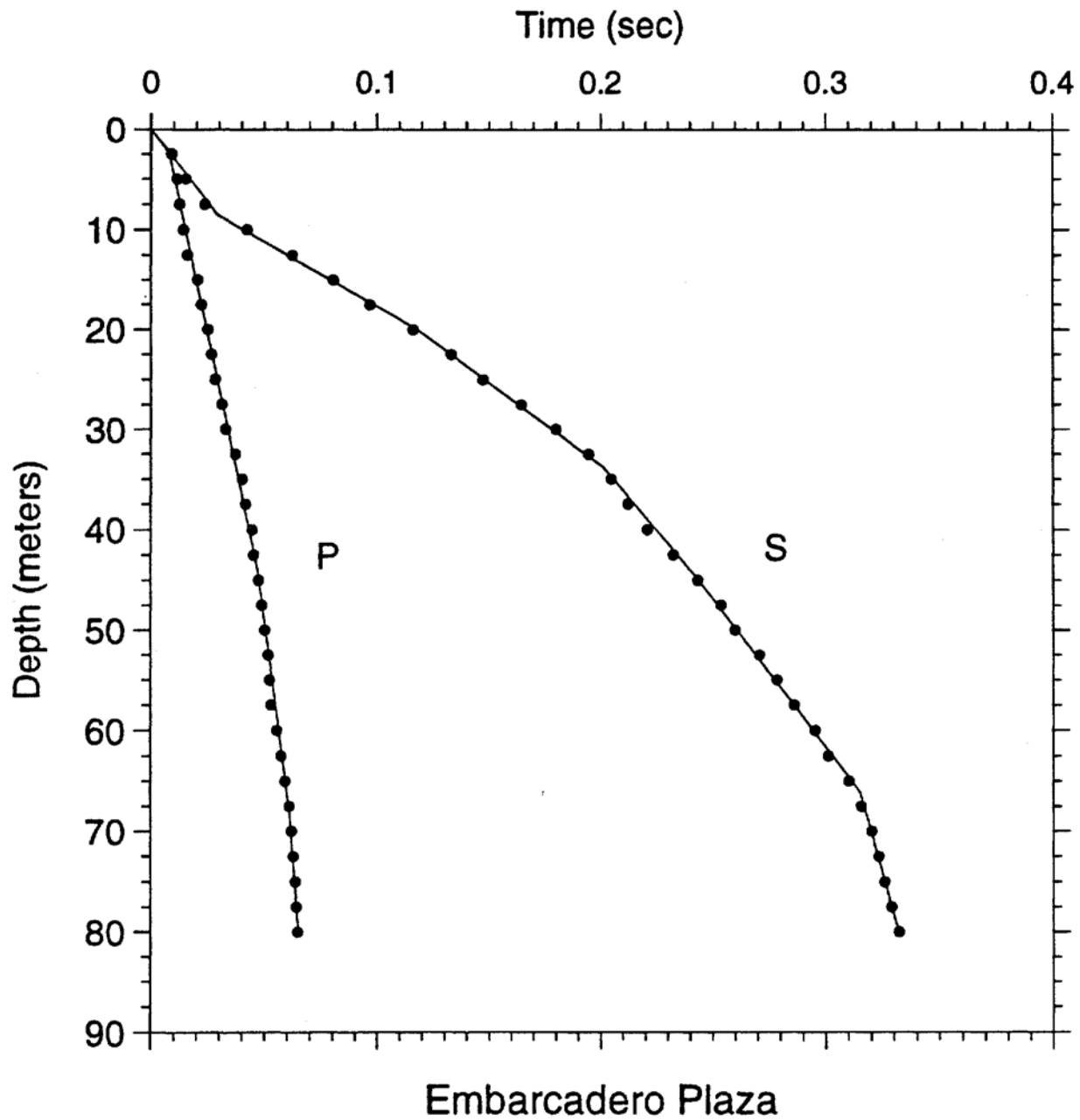


Figure B3. Time-depth graph of P-wave and S-wave picks. Line segments show the hinged-least-squares fit to the data points.

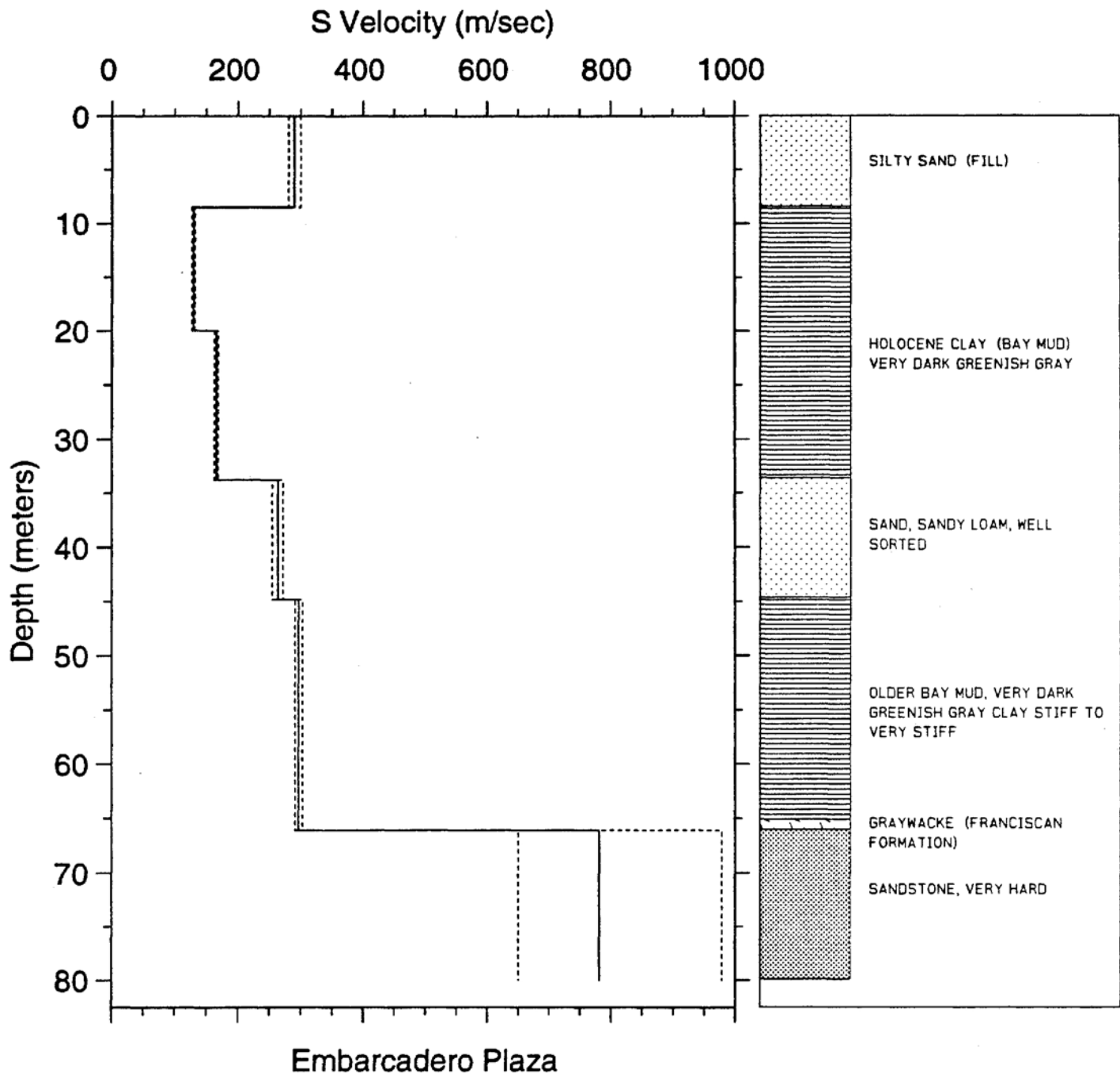


Figure B4a. S-wave velocity profiles with dashed lines representing plus and minus one standard deviation. Simplified geologic log is shown for correlation with velocities.

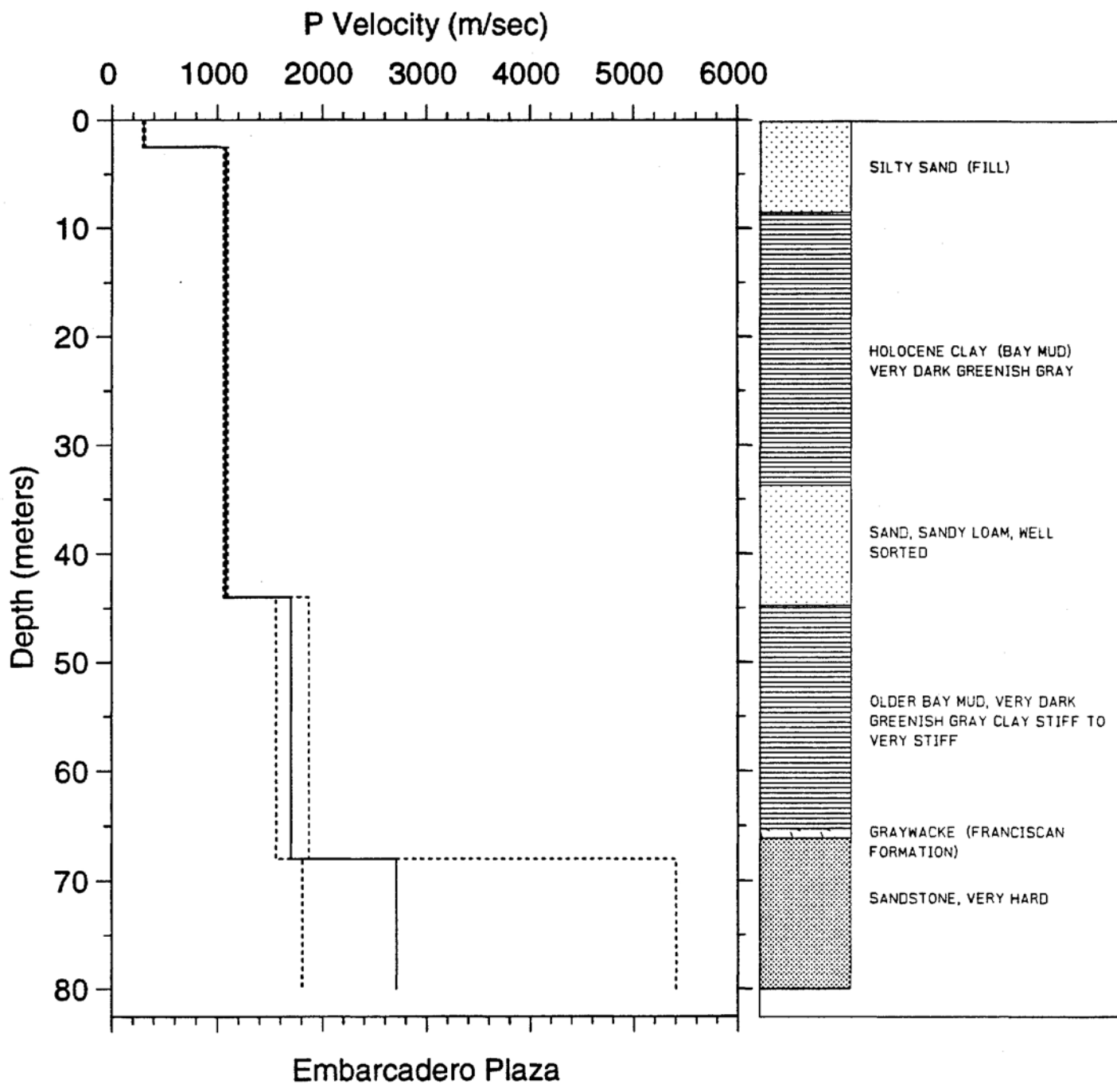


Figure B4b. P-wave velocity profiles with dashed lines representing plus and minus one standard deviation. Simplified geologic log is shown for correlation with velocities.

TABLE B1a. S-wave arrival times and velocity summaries for Embarcadero Plaza site.

d(m)	d(ft)	t(sec)	sig	rsdl/sig	dtb(m)	dtb(ft)	ttb(s)	v(m/s)	vl(m/s)	vu(m/s)	v(ft/s)	vl(ft/s)	vu(ft/s)
2.5	8.2	.0092	1	.6	.0	.0	.000						
5.0	16.4	.0153	1	-1.9	8.5	27.9	.029	290	281	300	952	922	984
7.5	24.6	.0236	1	-2.3	20.0	65.6	.118	130	128	132	426	420	434
10.0	32.8	.0424	1	1.6	33.8	110.9	.201	166	163	169	544	535	553
12.5	41.0	.0623	1	2.2	44.8	147.0	.243	264	255	272	865	838	893
15.0	49.2	.0805	1	1.2	66.1	216.9	.315	297	291	303	974	956	993
17.5	57.4	.0969	1	-1.6	80.0	262.5	.332	781	650	978	2562	2133	3208
20.0	65.6	.1162	1	-1.6									
22.5	73.8	.1331	1	.2									
25.0	82.0	.1474	1	-.5									
27.5	90.2	.1646	1	1.6									
30.0	98.4	.1799	1	1.8									
32.5	106.6	.1947	1	1.5									
35.0	114.8	.2047	1	-.9									
37.5	123.0	.2123	1	-2.8									
40.0	131.2	.2210	2	-1.8									
42.5	139.4	.2325	1	-1.6									
45.0	147.6	.2433	1	-.2									
47.5	155.8	.2536	1	1.7									
50.0	164.0	.2599	1	-.4									
52.5	172.2	.2707	1	2.0									
55.0	180.4	.2786	3	.5									
57.5	188.6	.2861	1	.5									
60.0	196.9	.2954	1	1.4									
62.5	205.1	.3011	1	-1.3									
65.0	213.3	.3101	1	-.7									
67.5	221.5	.3156	1	-.7									
70.0	229.7	.3201	3	.2									
72.5	237.9	.3233	2	.3									
75.0	246.1	.3258	3	.0									
77.5	254.3	.3291	4	.0									
80.0	262.5	.3322	4	.0									

31

Explanation:

d(m) = depth in meters

d(ft) = depth in feet

t(sec) = arrival time in seconds (S-wave arrival times are the average of picks from traces obtained from hammer blows differing in direction by 180°)

sig = sigma, standard deviation normalized to the standard deviation of best picks

rsdl/sig = least-squares residual divided by sigma

dtb(m) = depth to bottom of layer in meters

dtb(ft) = depth to bottom of layer in feet

ttb(s) = arrival time in seconds to bottom of layer

v(m/s) = velocity in meters per second

vl(m/s) = lower limit of velocity in meters per second \*

vu(m/s) = upper limit of velocity in meters per second

v(ft/s) = velocity in feet per second

vl(ft/s) = lower limit of velocity in feet per second

vu(ft/s) = upper limit of velocity in feet per second

\* see text for explanation of velocity limits

TABLE B1b. P-wave arrival times and velocity summaries for Embarcadero Plaza site.

d(m)	d(ft)	t(sec)	sig	rsdl/sig	dtb(m)	dtb(ft)	ttb(s)	v(m/s)	vl(m/s)	vu(m/s)	v(ft/s)	vl(ft/s)	vu(ft/s)
2.5	8.2	.0090	1	.7	.0	.0	.000						
5.0	16.4	.0115	1	.9	2.5	8.2	.008	302	292	314	992	958	1029
7.5	24.6	.0125	1	-.4	44.0	144.4	.047	1080	1061	1099	3542	3480	3607
10.0	32.8	.0143	1	-.9	68.0	223.1	.061	1701	1559	1870	5579	5116	6134
12.5	41.0	.0160	1	-1.5	80.0	262.5	.065	2710	1808	5405	8890	5932	17732
15.0	49.2	.0206	1	.8									
17.5	57.4	.0222	1	.0									
20.0	65.6	.0252	1	.7									
22.5	73.8	.0267	3	.0									
25.0	82.0	.0283	1	-.8									
27.5	90.2	.0313	3	.0									
30.0	98.4	.0328	1	-.9									
32.5	106.6	.0373	1	1.2									
35.0	114.8	.0403	5	.4									
37.5	123.0	.0419	5	.2									
40.0	131.2	.0447	4	.4									
42.5	139.4	.0454	4	.0									
45.0	147.6	.0475	4	.1									
47.5	155.8	.0489	4	.0									
50.0	164.0	.0503	4	.0									
52.5	172.2	.0517	4	.0									
55.0	180.4	.0524	4	-.2									
57.5	188.6	.0530	4	-.4									
60.0	196.9	.0557	4	-.1									
62.5	205.1	.0575	4	.0									
65.0	213.3	.0593	4	.1									
67.5	221.5	.0611	4	.1									
70.0	229.7	.0620	4	.1									
72.5	237.9	.0629	4	.1									
75.0	246.1	.0638	4	.1									
77.5	254.3	.0643	4	.0									
80.0	262.5	.0648	4	-.1									

Explanation:

d(m) = depth in meters

d(ft) = depth in feet

t(sec) = arrival time in seconds (S-wave arrival times are the average of picks from traces obtained from hammer blows differing in direction by 180°)

sig = sigma, standard deviation normalized to the standard deviation of best picks

rsdl/sig = least-squares residual divided by sigma

dtb(m) = depth to bottom of layer in meters

dtb(ft) = depth to bottom of layer in feet

ttb(s) = arrival time in seconds to bottom of layer

v(m/s) = velocity in meters per second

vl(m/s) = lower limit of velocity in meters per second \*

vu(m/s) = upper limit of velocity in meters per second

v(ft/s) = velocity in feet per second

vl(ft/s) = lower limit of velocity in feet per second

vu(ft/s) = upper limit of velocity in feet per second

\* see text for explanation of velocity limits

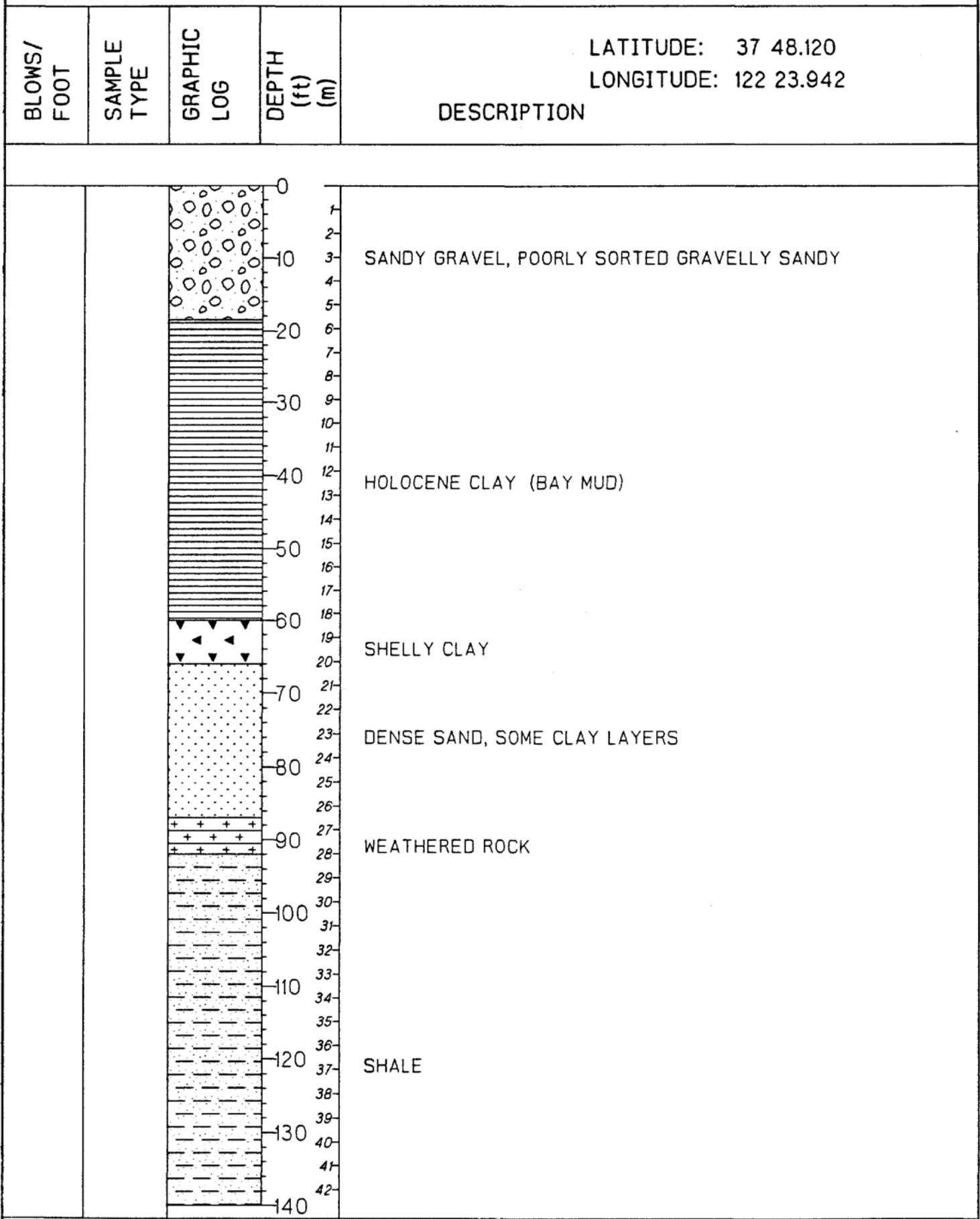


Figure C1. Geologic log of Levi Plaza borehole. 33

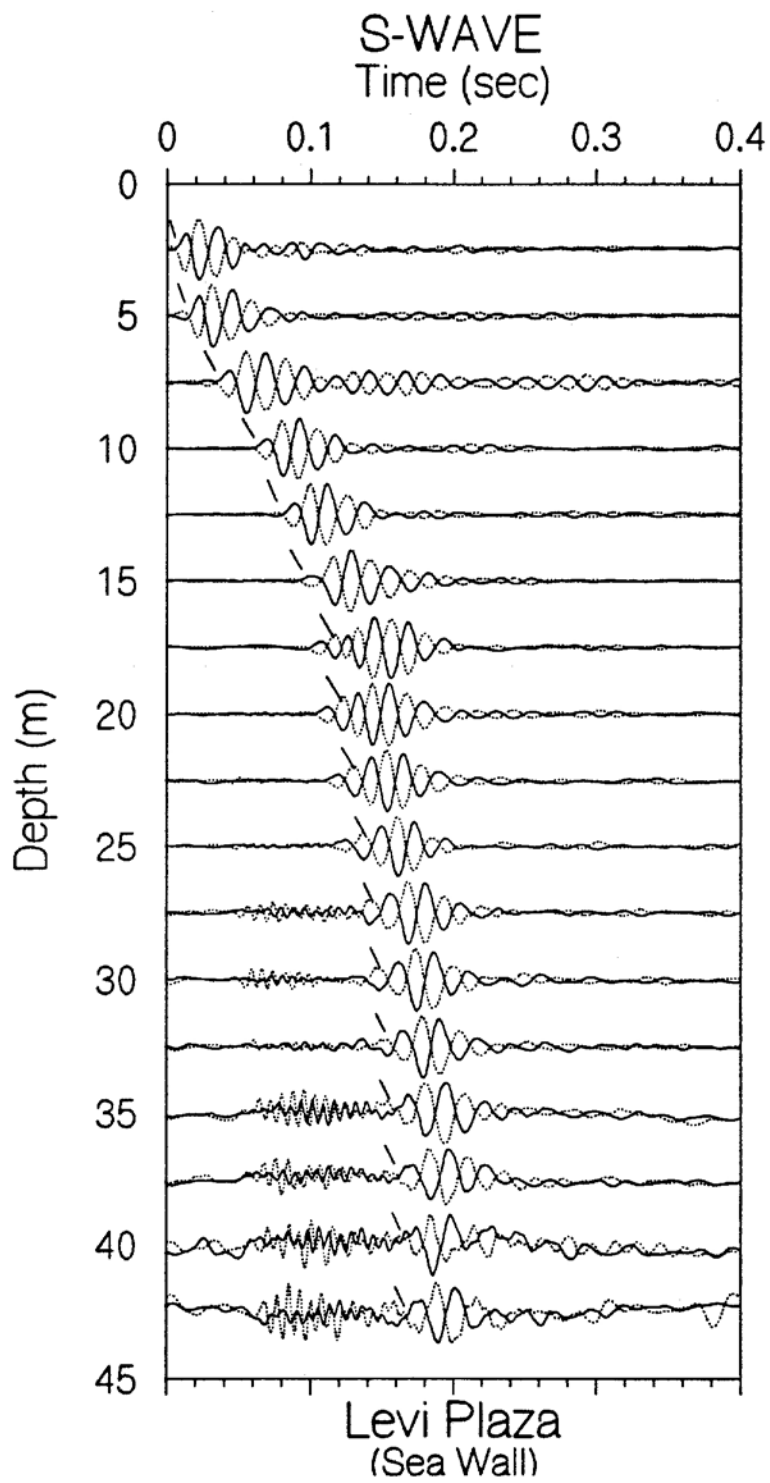


Figure C2a. Horizontal-component record section (from horizontal impacts in opposite directions) superimposed for identification of S-wave onset. Approximate S-wave picks are indicated by the accent marks.

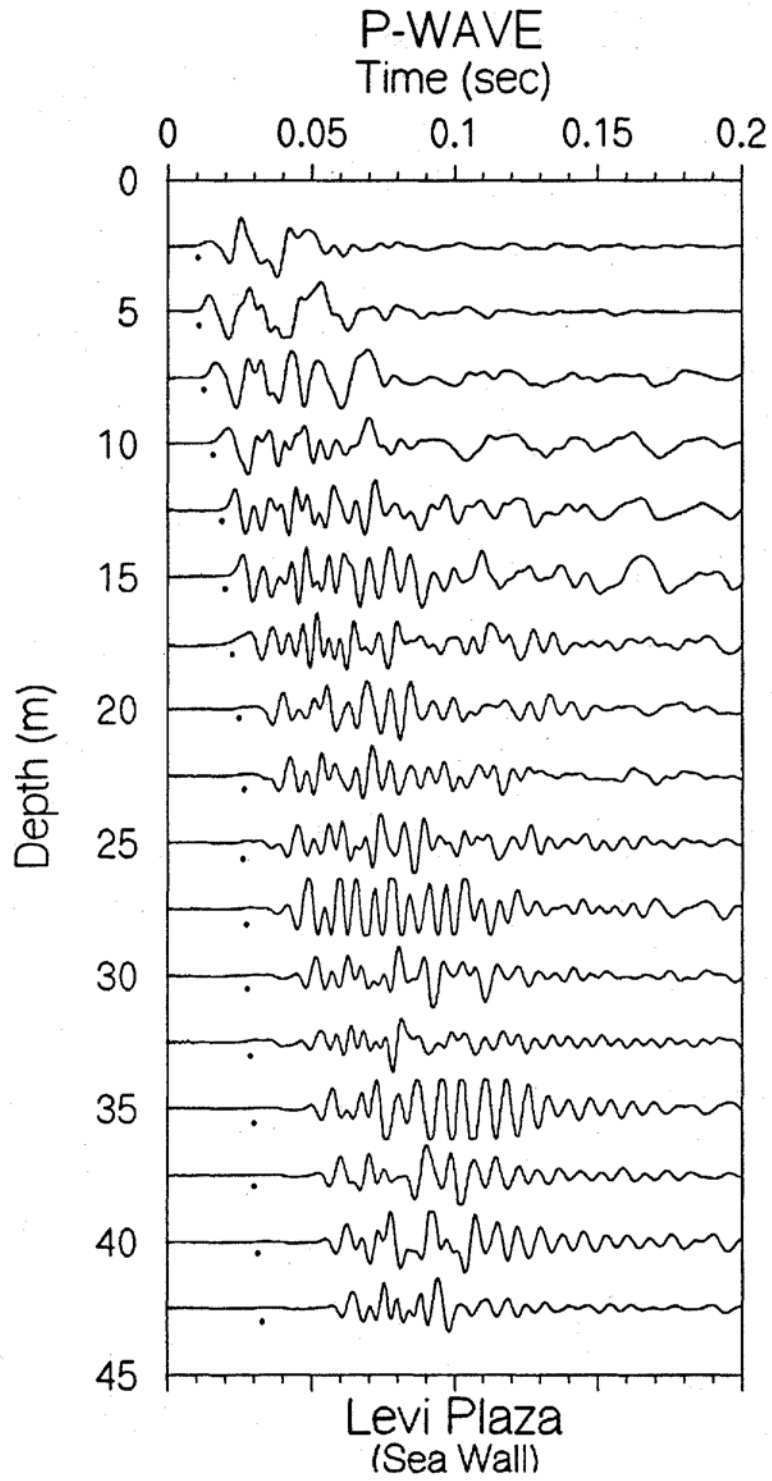


Figure C2b. P-wave record section. Approximate P-wave picks are shown by the dots.

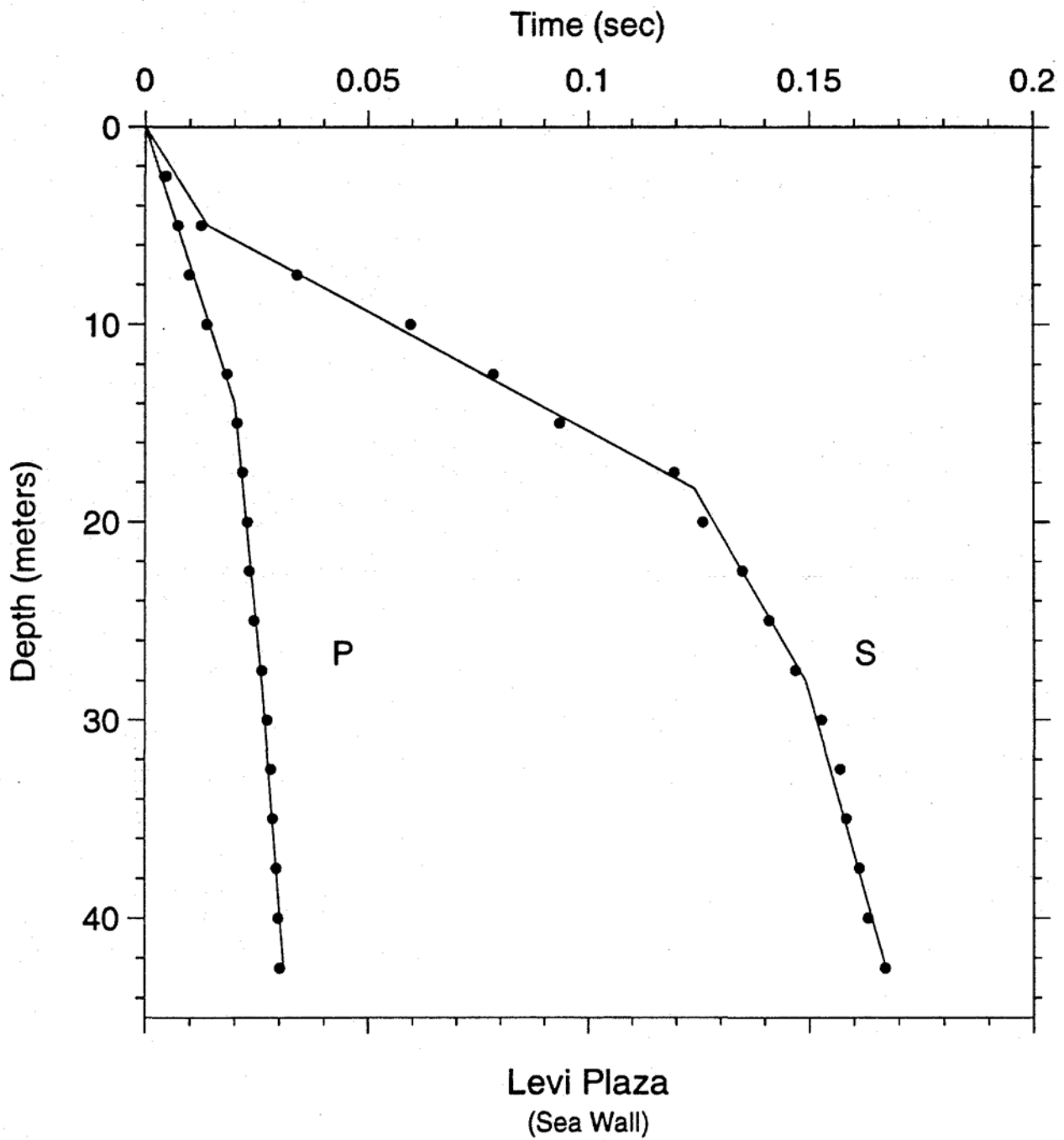


Figure C3. Time-depth graph of P-wave and S-wave picks. Line segments show the hinge-least-squares fit to the data.

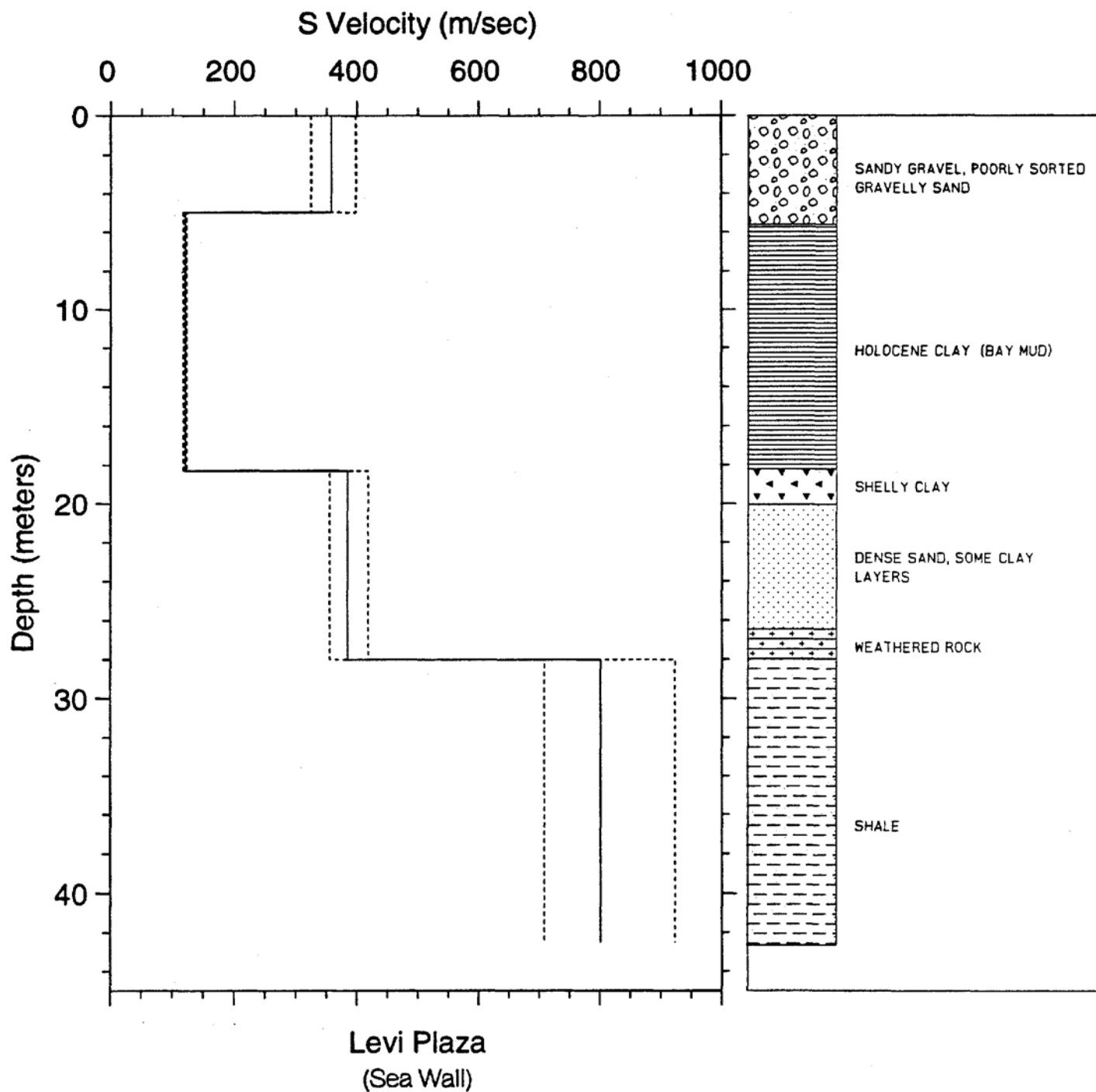


Figure C4a. S-wave velocity profiles with dashed lines representing plus and minus one standard deviation. Simplified geologic log is shown for correlation with velocities.

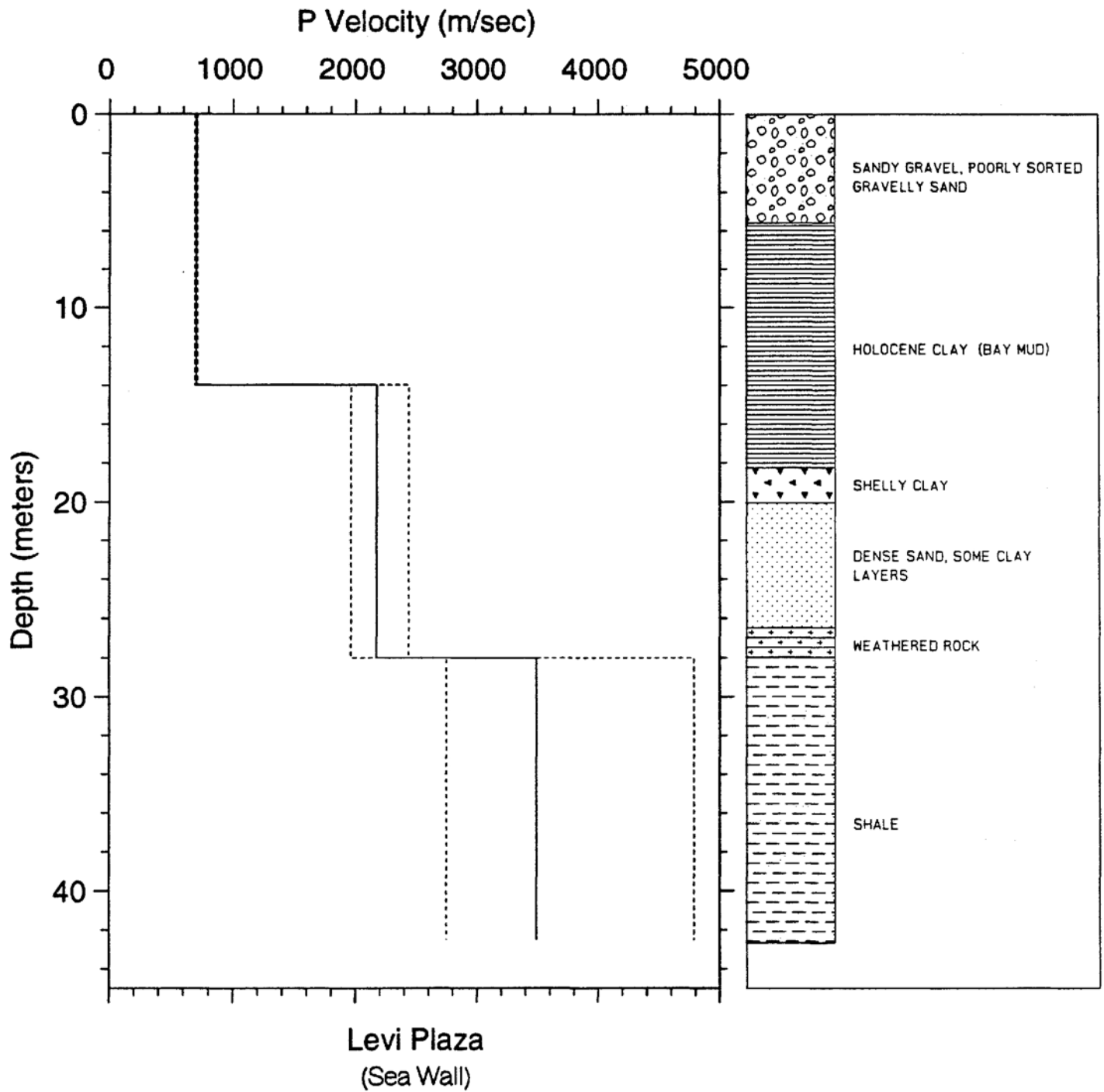


Figure C4b. P-wave velocity profiles with dashed lines representing plus and minus one standard deviation. Simplified geologic log is shown for correlation with velocities.

TABLE C1a. S-wave arrival times and velocity summaries for Levi Plaza site.

d(m)	d(ft)	t(sec)	sig	rsdl/sig	dtb(m)	dtb(ft)	ttb(s)	v(m/s)	vl(m/s)	vu(m/s)	v(ft/s)	vl(ft/s)	vu(ft/s)
2.5	8.2	.0048	1	-2.2	.0	.0	.000						
5.0	16.4	.0126	1	-1.4	5.0	16.4	.014	358	325	398	1174	1067	1305
7.5	24.6	.0340	1	-.7	18.3	60.0	.124	121	118	123	396	389	405
10.0	32.8	.0596	1	4.2	28.0	91.9	.149	384	355	418	1260	1166	1371
12.5	41.0	.0784	1	2.4	42.5	139.4	.167	801	708	923	2629	2322	3029
15.0	49.2	.0935	1	-3.2									
17.5	57.4	.1195	1	2.1									
20.0	65.6	.1260	1	-2.5									
22.5	73.8	.1349	1	-.1									
25.0	82.0	.1409	1	-.6									
27.5	90.2	.1468	1	-1.2									
30.0	98.4	.1526	1	.8									
32.5	106.6	.1568	1	1.9									
35.0	114.8	.1582	1	.2									
37.5	123.0	.1611	1	-.1									
40.0	131.2	.1631	2	-.6									
42.5	139.4	.1669	1	-.5									

Explanation:

d(m) = depth in meters

d(ft) = depth in feet

t(sec) = arrival time in seconds (S-wave arrival times are the average of picks from traces obtained from hammer blows differing in direction by 180°)

sig = sigma, standard deviation normalized to the standard deviation of best picks

rsdl/sig = least-squares residual divided by sigma

dtb(m) = depth to bottom of layer in meters

dtb(ft) = depth to bottom of layer in feet

ttb(s) = arrival time in seconds to bottom of layer

v(m/s) = velocity in meters per second

vl(m/s) = lower limit of velocity in meters per second \*

vu(m/s) = upper limit of velocity in meters per second

v(ft/s) = velocity in feet per second

vl(ft/s) = lower limit of velocity in feet per second

vu(ft/s) = upper limit of velocity in feet per second

\* see text for explanation of velocity limits

66

TABLE C1b. P-wave arrival times and velocity summaries for Levi Plaza site.

d(m)	d(ft)	t(sec)	sig	rsdl/sig	dtb(m)	dtb(ft)	tth(s)	v(m/s)	vl(m/s)	vu(m/s)	v(ft/s)	vl(ft/s)	vu(ft/s)
2.5	8.2	.0044	1	.8	.0	.0	.000						
5.0	16.4	.0074	1	.3	14.0	45.9	.020	700	692	709	2298	2272	2325
7.5	24.6	.0099	1	-.8	28.0	91.9	.026	2174	1962	2437	7132	6436	7996
10.0	32.8	.0138	1	-.5	42.5	139.4	.031	3491	2747	4788	11453	9011	15710
12.5	41.0	.0183	1	.5									
15.0	49.2	.0206	1	.2									
17.5	57.4	.0218	3	.1									
20.0	65.6	.0229	3	.1									
22.5	73.8	.0233	3	-.2									
25.0	82.0	.0244	3	-.2									
27.5	90.2	.0261	3	.0									
30.0	98.4	.0273	3	.1									
32.5	106.6	.0282	3	.2									
35.0	114.8	.0286	3	.1									
37.5	123.0	.0294	3	.1									
40.0	131.2	.0298	3	.0									
42.5	139.4	.0302	3	-.1									

Explanation:

d(m) = depth in meters

d(ft) = depth in feet

t(sec) = arrival time in seconds (S-wave arrival times are the average of picks from traces obtained from hammer blows differing in direction by 180°)

sig = sigma, standard deviation normalized to the standard deviation of best picks

rsdl/sig = least-squares residual divided by sigma

dtb(m) = depth to bottom of layer in meters

dtb(ft) = depth to bottom of layer in feet

tth(s) = arrival time in seconds to bottom of layer

v(m/s) = velocity in meters per second

vl(m/s) = lower limit of velocity in meters per second \*

vu(m/s) = upper limit of velocity in meters per second

v(ft/s) = velocity in feet per second

vl(ft/s) = lower limit of velocity in feet per second

vu(ft/s) = upper limit of velocity in feet per second

\* see text for explanation of velocity limits